ANALYSIS OF MISSILE IMPACT PROBABILITY FOR GENERIC TORNADO HAZARD ASSESSMENTS

Prepared for

U.S. Nuclear Regulatory Commission
Division of Risk Assessment of the
Office of Nuclear Reactor Regulation

Prepared by

Osvaldo Pensado

Southwest Research Institute®
Center for Nuclear Waste Regulatory Analyses

July 29, 2016

ABSTRACT

The nuclear energy industry is considering defining a generic missile impact probability (number of hits per missile per unit of target area) to be used in support of tornado hazard assessments to multiple nuclear power plants. A tornado-generated missile (a missile for brief) is an object launched by high-speed tornado winds that have the potential to damage or fail a structure in a nuclear power plant. The hit frequency to a target structure would be estimated as linearly proportional to the tornado frequency, the number of missiles, the target area, and the missile impact probability. The hit frequency so computed for relevant safety significant components would be input to probabilistic risk assessments that estimate risk metrics such as core damage frequency and large early-release frequency. The missile impact probability (MIP) is proposed to be computed using data in the Tornado Missile Risk Analysis report (NP-768) published by the Electric Power Research Institute (1978). In this report the MIP concept is evaluated, and recommendations are provided to strengthen the technical basis of its use.

The NP-768 includes hit frequencies to buildings of hypothetical power plants. With those hit frequencies, the tornado frequencies, and building dimensions, MIP values were derived, and the dependence of the MIP on factors such as building dimensions, configuration of buildings in a plant, and spread of potential missiles was analyzed. The MIP was found to be independent of the value of the tornado frequency, but dependent on the tornado magnitude, the height of the target, the configuration of buildings in a plant (e.g., nearby buildings shield each other against missile hits), and the area of spread of the initial location of missiles. In addition, the NP-768 data suggest that missiles hitting tall buildings may carry more energy than missiles hitting targets close to the ground. It is concluded that the MIP concept is technically defensible. However, it is recommended to carefully select a reference MIP to minimize dependence on building configuration, and perform additional analyses to properly account for the initial spread and distance of missiles to a target. Correction factors are suggested to the MIP to account for different missile zones; however, those corrections may be overly conservative for cases in which the missile clusters are distant from a target.

Reference

EPRI. “Tornado Missile Risk Analysis.” Report NP-768. Electric Power Research Institute: Washington DC. May
1978. http://www.epri.com/abstracts/Pages/ProductAbstract.aspx?ProductId=NP-768

CONTENTS

FIGURES

TABLES

ACKNOWLEDGMENTS

This report was prepared to document work performed by the Center for Nuclear Waste Regulatory Analyses (CNWRA®) for the U.S. Nuclear Regulatory Commission (NRC) under Contract No. NRC–HQ–50–14–E–0001. The activities reported here were performed on behalf of the NRC Office of Nuclear Reactor Regulation, Division of Risk Assessment. The report is an independent product of CNWRA and does not necessarily reflect the views or regulatory position of the NRC. The author thanks Dr. Biswajit Dasgupta and Dr. John Stamatakos for their technical reviews, Lora Neill for her editorial review, and Leonora Naukam for secretarial support.

QUALITY OF DATA, ANALYSES, AND CODE DEVELOPMENT DATA

Tasks were executed under the established Geosciences and Engineering Division (GED) Quality Assurance (QA) Program, which is described in the GED QA Manual, approved by the NRC, and audited for compliance annually. This QA program is implemented t through Administrative Procedures (APs), Quality Assurance Procedures (QAPs), and Technical Operating Procedures (TOPs). Specific GED QA procedures that apply to this project include QAP–002, Review of Documents, Reports, and Papers; and QAP–014, Documentation and Verification of Scientific and Engineering Calculations. Appropriate APs also have been used, as necessary (e.g., evaluations of potential for conflict of interest).

DATA: All CNWRA-generated original data contained in this report meet the QA requirements described in the CNWRA QA Manual. Each data source is cited in this report, as appropriate, and should be consulted for determining the level of quality for those cited data. Data from the Missile Risk Analysis report (NP-768) published by the Electric Power Research Institute (1978) were used in the analysis in this report. The majority of the data used are tabulated in this report, and detailed instructions are provided to reproduce simple arithmetic computations.

ANALYSES AND CODES: The calculations presented in this report were performed using Excel® and Mathematica®. Electronic files were archived with this report.

Reference

EPRI. "Tornado Missile Risk Analysis." Report NP-768. Electric Power Research Institute: Washington DC. May
1978. http://www.epri.com/abstracts/Pages/ProductAbstract.aspx?ProductId=NP-768

1 INTRODUCTION

The nuclear energy industry is currently analyzing external hazards challenging the safety of the operation of facilities from tornadoes. The primary scenario of concern is one in which a tornado forms near or traversing across a nuclear power plant facility and the high-speed tornado winds launch large objects (referred to as *missiles*) into the tornado wind field which strike and damage structures (such as exhaust stacks, cable vaults, access doors, and tanks) that are not explicitly designed to withstand these kinds of high-energy impacts.

To facilitate the analysis of tornado hazards within a risk-informed and performance-based approach to evaluating plant safety, the nuclear energy industry is proposing to define a missile impact probability (MIP) parameter based on 1978 tornado missile risk analyses sponsored by the Electric Power Research Institute (EPRI, 1978). The MIP would be directly scaled with factors accounting for the tornado frequency, the number of missiles in or near a facility, and the area of a safety-related component to estimate the hit frequency to that component. The goal of the nuclear energy industry is to estimate initiating event frequencies that can be input into an external events probabilistic risk assessment (PRA) model that calculates core damage frequency (CDF) and large early-release frequency (LERF).

In this report, we evaluate the MIP concept and the scaling approach to apply to multiple nuclear power plant sites. The objective of this report is to analyze the dependencies of MIP on variables such as target geometry, target placement, and the initial distribution of missiles. The goal is to provide an assessment of the approach to scale the MIP to estimate the hit frequency to be used in tornado risk assessments of different plant sites. The analysis considered data in tables of the NP-768 Tornado Missile Risk Analysis report (EPRI, 1978) as a way to identify trends, correlations, and dependencies of the MIP. The data required simple arithmetic operations to derive MIP values. The majority of the data used to reproduce plots in this report are provided in tables. In other cases, the approach to reproduce those plots from straightforward manipulation of the NP-768 data is described in detail. It is noted that the NP-768 report documents only limited results. Results are provided in tables, and other results are only qualitatively discussed in the text. Because of the limited data in NP-768, some discussion in this report is also qualitative, but visuals are included when possible to support and clarify conclusions.

The report is organized in four chapters. Chapter 1 defines basic concepts, such as the tornado strike frequency and the MIP parameter. Chapter 2 documents the main analysis, organized in sections exploring the dependence of MIP on tornado frequency, the geometry of targets and relative placement of those targets (i.e., mutual shielding), tornado intensity, and the initial missile spread. The last section of Chapter 2 analyzes the energy of the missiles strikes and whether it is appropriate to take credit for the structural strength of targets against missile impacts. Chapter 3 provides the conclusions, and Chapter 4 lists the references.

1.1 Summary of EPRI NP-768 Report Computations

In 1978, EPRI published a report titled Tornado Missile Risk Analysis (EPRI, 1978), documenting development of the TORMIS code to analyze the problem of tornados striking nuclear power facilities, with high-speed winds launching missiles and striking site buildings. This report is referred throughout as NP-768 (report number assigned by EPRI). EPRI considered multiple scenarios of tornados striking a site. Tornados were considered to take multiple alternative paths and be of different intensity. To explore the effect on missile hit frequencies of sites located in different places in the country, average tornado frequency of

three U.S. Nuclear Regulatory Commission (NRC) tornado regions (Regions I, II, and III, numbered in decreasing order of tornado frequencies) were used as input to the EPRI calculations. The calculations also explored effects of different missile types, different initial missile insertion heights, different initial locations of missiles through the site, and different configurations of buildings in the power plant. To study the different alternatives, the EPRI analysis was developed using a Monte Carlo approach with stratified and importance sampling, to sample quantities such as wind speeds and initial missile locations and insertion heights. EPRI examined statistical convergence on target hit frequencies, to select a sufficiently large sample of tornado paths and intensities (measured in a modified, F', Fujita scale) and missile trajectories. EPRI analyzed effects of different power plant buildings, by considering two hypothetical nuclear power plants, referred to as Plants A and B. The targets selected for the computation of hit frequencies were the buildings of the Plants A and B. Power Plant A was a single-unit plant with seven buildings. Plant B was a 2-unit plant with 16 buildings. Plant B was analyzed in two configurations: configuration B1 imagined that all unit 2 buildings were under construction when the tornado struck (with construction material providing a source of missiles). Configuration B2 imagined both units operational. The types of missiles considered included wood beams, pipes, steel rods, utility poles, plates, and automobile vehicles (cars and trucks). At Plant A, the missiles were assumed to be distributed uniformly over an enclosing area spanning 4,640 ft × 5,000 ft (= 2.32×10^7 ft^2). For Plant B, the distribution of missiles was non-uniform in the B1 and B2 configurations, including different assumptions on insertion heights and the initial location of missile types (e.g., vehicles were predominantly located in parking lots). Using the TORMIS code, missile trajectories were simulated and the characteristics of the hits on the different buildings or targets were recorded (such as impact speeds and scabbing damage). Statistics were derived to quantify the number of hits per target, the number of hits per missile, the number of hits with specific features (including whether a threshold velocity was exceeded or whether a given amount of damage was caused by the hit), and associated hit frequencies.

The nuclear energy industry is proposing to rely on aspects of the EPRI analyses to support its current analysis of tornado hazards at specific plant sites, by defining a MIP based on the hit frequencies per missile, tornado frequencies, and target dimensions that can be abstracted from the data reported in NP-768. Moreover, although the targets evaluated in NP-768 were large buildings, the nuclear energy industry is proposing an area-scaling approach in order to estimate the number of hits and hit frequency on all targets of interest, including small area targets such as exhaust stacks, cable vaults, access doors, and tanks.

1.2 Point-Strike Frequency and Area-Strike Frequency

Two important parameters needed to understand the NP-768 analyses are the point-strike frequency and area-strike frequency. NUREG/CR–4461 (Ramsdell and Rishel, 2007) defines the tornado point-strike frequency as

$$f_{point} = \frac{N\, A_t}{T\, A_r} \qquad [1]$$

f_{point} – tornado point-strike frequency
A_r – area of land in a square 2° × 2° enclosing the facility
A_t – average damage area per tornado
N – number of recorded tornados on the 2° × 2° square over a period T
T – time of record of the tornado strikes

The point-strike frequency is the expected tornado-damage area fraction per year. The tornado damage area, A_t, is computed as

$$A_t = w_t L_t \quad [2]$$

w_t – tornado width
L_t – tornado length

If the dimensions of the facility are significant, Eq. [1], is modified as follows

$$f_{area} = \frac{N\ (w_t\ + w_s)\ L_t}{T\ A_r} \quad [3]$$

where w_s is a characteristic length of the facility or structure. The frequency f_{area} is referred to as tornado area-strike frequency. In the limit, when the structure is large (i.e., w_s is much larger than w_t), Eq. [3] can be approximated as

$$f_{area} = \frac{N\ w_s\ L_t}{T\ A_r} \quad [4]$$

which is equivalent to Eq. (4-6) in NUREG/CR–4461. NUREG/CR–4461 refers to Eq. [4] as including a "life-line" term to account for the structure dimensions. Note that

$$\frac{f_{area}}{f_{point}} = \frac{w_t\ + w_s}{w_t} = 1 + \frac{w_s}{w_t} > 1 \quad [5]$$

In other words, $f_{area} > f_{point}$. It is clear that the area-strike frequency is larger than the point-strike frequency because the larger dimensions of the facility increase the probability for a facility or structure to be struck by a tornado.

1.3 Definition of the Missile Impact Probability

The document NP-768 relies on the TORMIS code to compute missile hit frequencies for a number of targets (buildings of hypothetical nuclear power plants, Plants A and B) as function of the NRC tornado region frequency, the specific target, and the F' tornado scale.[1] H_i denotes the hit frequency per missile for target i. According to a presentation by the nuclear energy industry during a public meeting on March 23 (Montgomery, 2016), the MIP for target i, MIP_i^{NP}, is defined as

$$MIP_i^{NP} = \frac{H_i^{NP}}{f^{NP}\ A_i^{NP}} \quad [6]$$

[1]The standard tornado intensity scale in 1978 (year of publication of NP-768) was the Fujita (F) scale. The F' tornado scale was developed to attempt addressing known inconsistencies between tornado windspeeds in the F scale. The Enhanced Fujita (EF) scale is the current standard scale for tornado intensity; although the F' and EF scales are not identical, they are similar.

The superscript NP is used in this report to highlight quantities explicitly listed in NP-768 (or derived in straightforward manner from data therein). The term f^{NP} is the tornado frequency, H_i^{NP} is the hit frequency per missile (i.e., the ratio of the hit frequency to the number of missiles) and A_i^{NP} is the area of target i. The nuclear energy industry is proposing using a generalized MIP value for use in safety analyses of tornado impacts. Given a reference MIP computed on the basis of data in NP-768 (denoted as MIP^{NP}) and a site tornado frequency equal to f, the nuclear energy industry is proposing computing the initiating event frequency, f_{ie}, as

$$f_{ie} = f\ MIP^{NP}\ \times (\text{number of missiles}) \times (\text{area of target}) \qquad [7]$$

The quantity $f\ MIP^{NP}\ \times (\text{number of missiles}) \times (\text{area of target})$ is an estimate of the hit frequency to a site-specific target. The number of missiles may be identified by surveys of the nuclear power plant site. The target may be a safety-relevant component, and the area may be a pertinent cross section in the line-of-sight of a potential tornado-generated missile. The nuclear energy industry is proposing to assume that that any missile hit would fail the target or component (i.e., the industry conservatively assumes a failure probability = 1 no matter how energetic the hit). Because of this assumption the hit frequency is equated to a failure frequency of the safety-relevant component. In Chapter 2 dependencies of the MIP are examined, as well as strengths and limitations of the scaling approach.

2 ANALYSIS OF THE MISSILE IMPACT PROBABILITY PARAMETER

The objective of this chapter is to examine dependencies of the missile impact probability (MIP) and the scaling approach proposed by the nuclear energy industry, summarized in Eq. [7]. Questions such as the following are considered

- Is the MIP dependent on the tornado region where the plant is located?
- Does the approach to compute the tornado frequency (e.g., area strike or point strike) change the scaling approach in Eq. [7]?
- Does the distribution of buildings in a nuclear power plant, and the geometry and dimensions of those buildings, affect the MIP?
- Is the MIP a function of the tornado intensity?
- What is the relationship of features of missiles (e.g., initial location and initial insertion height) to the MIP and the scaling approach (Eq. [7])?
- Is there information in NP-768 that may allow justifying taking credit for the structural strength of targets against failure?
- What is a reasonable reference value of MIP to be used in generic tornado hazard analyses?

By examining possible answers to those questions, the technical bases for using a single reference MIP to be used in multiple nuclear power plant sites are evaluated. To deal with the posed questions, the analysis in this chapter is organized in sections that examine the dependence of MIP on tornado frequency, the geometry of targets and mutual shielding among those targets, tornado intensity, and the missile spread. The distribution of energy of the hitting missiles is briefly analyzed to explore the potential for of taking at least partial credit for the strength of target to absorb tornado missile impacts without damage or failure. Suggestions on possible values to use as reference MIP are provided.

2.1 The Hit Frequency Is Linearly Proportional to the Tornado Frequency

This section examines the questions

- Is the MIP dependent on the tornado region where the plant is located?
- Does the approach to compute the tornado frequency (e.g., area strike or point strike) change the nuclear energy industry scaling approach in Eq. [7]?

Data from NP-768 were examined, and we concluded that the MIP is independent of the NRC tornado region. Estimating the tornado frequency using area-strike or point-strike concepts, or other alternatives, would not change the MIP. No adjustments would be needed to use Eq. [7] if different alternatives to estimate tornado frequencies were adopted. The detailed analysis to derive these conclusions follows.

Table 3-15 in NP-768 lists total hit frequencies per missile, H, for three tornado regions and for tornado intensities from F'2 to F'6 for the hypothetical Plant A. The hit frequency per missile H_i

for target i is the number of missile hits per year divided by the total number of missiles considered in the analysis. The total hit frequency per missile, H_T, for Plant A (consisting of seven buildings or targets) is defined as

$$H_T = \sum_{i=1}^{7} H_i^{NP} \qquad [8]$$

The quantity H_T is a function of the tornado region and of the F' tornado intensity scale. Values (low bound, mean, and upper bound) of H_T as a function of F' are listed in NP-768, Table 3-15. Figure 1 compares the ratio H_T/f^{NP} for the three regions and F'2 to F'5 tornado intensity computed for Plant A. Trend lines are included to enhance the visual comparison. The F'6 values are not included, because only Region I would be affected by F'6 tornados. Mean values for the tornado frequency f^{NP} were obtained from NP-768, Table 3-4. Table 3-4 defines confidence intervals on the frequency (interpreted as confidence on the mean frequency). For each region, three curves are provided in Figure 1 representing the low limit, mean curve, and the upper limit. The ratios H_T/f^{NP} are essentially the same for the three tornado regions, demonstrating that the total hit frequency per missile, H_T, is linearly proportional to the tornado frequency. Differences are noted between Region I and Region II only at F'5 tornado intensity, and between Region I and Region III only at F'4 intensity. Those differences are most likely statistical artifacts, expected to become minor or null if the statistical population of tornados and missiles was increased in the TORMIS computations.

We confirmed that the ratio H_i^{NP}/f^{NP} is the same for any given target and tornado intensity, and independent of the numeric value of the frequency f^{NP}. The H_i^{NP} frequencies are listed in NP-768, Tables 3-8 to 3-14 (for Targets 1 to 7), as function of the tornado intensity and tornado region. In other words, in similitude to Figure 1, for a fixed target i and fixed F' intensity, the ratio H_i^{NP}/f^{NP} is the same for all of the NRC tornado regions (except for possible statistical artifacts). Furthermore for a fixed target i, the ratio H_i^{NP}/f^{NP} is independent of the NRC tornado region for the Plant B in B1 and B2 configurations.

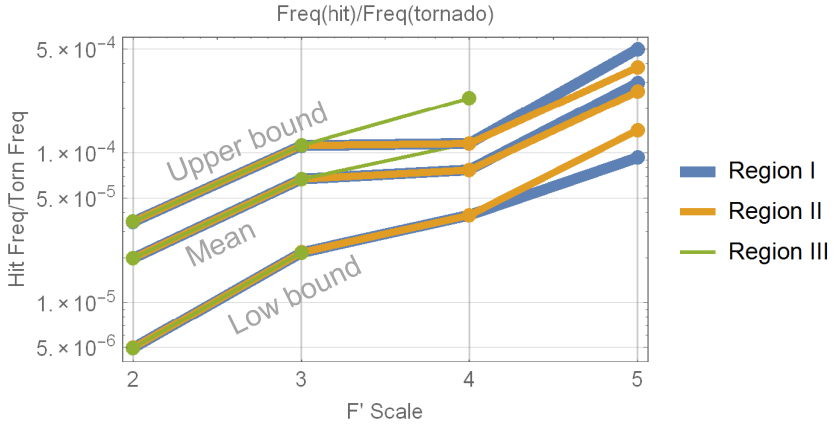

Figure 1. Number of Hits per Missile, H_T/f^{NP}, as a Function of the Tornado Intensity and the NRC Tornado Region. The Three Trend Lines per Region Represent Low, Mean, and Upper Bounds. Differences Among the Three Regions Are Suspected Solely Due to Statistical Artifacts. H_T Data Are From NP-768, Table 3-15. Mean Values of the Frequency f^{NP} Were Obtained From NP-768, Table 3-4.

The information in NP-768 supports our conclusion that the ratios H_T/f^{NP} and H_i^{NP}/f^{NP} are independent of tornado frequency. The ratio H_i^{NP}/f^{NP} is interpreted as the number of hits per missile for target i, given a tornado at or near a site. Based on the NP-768 data, the quantity H_i can be defined as

$$H_i^{NP} = f^{NP} \frac{h_i}{M_s} \quad [9]$$

f^{NP} – tornado frequency
h_i – number of hits on target i
M_s – total number of missiles in the analysis

The quantity h_i is not explicitly specified in the NP-768. The total number of missiles, M_s, is defined in NP-768; however, the ratio h_i/M_s is independent of M_s. Thus, adding a superscript NP to M_s is not needed. Under the definition in Eq. [9], the ratio H_i^{NP}/f^{NP} is independent of tornado frequency. On the other hand, as discussed in the next sections, this ratio depends on tornado intensity. The TORMIS code appears not to simulate regional differences of tornado features (because if it did, the ratios H_T/f^{NP} and H_i^{NP}/f^{NP} would vary from region to region). A tornado of a given F' intensity is identical in all of the regions. The missile speeds and trajectories are identical from region to region. A tornado of defined intensity will produce exactly the same number of hits h_i (assuming the same number total number of missiles, M_s, are available in the analysis), regardless of the NRC tornado region. Thus, MIP is independent of the NRC tornado region and of the numeric value of the frequency.

We concluded that the hit frequency per missile for a target i, H_i, is linearly proportional to tornado frequency. If the tornado frequency increased by a factor of two, the hit frequency would also increase by two. In other words, the ratio H_i/f is independent of the numeric value of the tornado frequency f. An important corollary to this finding is the following. If the tornado frequency changes from point-strike to area-strike, the ratio H_i/f computed with data generated from detailed TORMIS runs would remain the same. Therefore, there is no need to introduce conversion factors to transform MIP from point-strike to area-strike frequency.

A probabilistic risk assessment of tornado-generated missile impact on the Calvert Cliffs Nuclear Power (Calvert Cliffs NPP, 1994) asserts that the tornado frequency in NP-768 is based on area-strike frequency. In the Calvert Cliffs analysis, an adjustment factor to the MIP (the MIP is denoted with the symbol Ψ in the Calvert Cliffs document) with respect to values derived from NP-768 data was used to account for changes in the tornado frequency. The area-strike frequency for the Calvert Cliffs site was computed with a smaller characteristic length (smaller than the site of 2,000-ft radius in the NP-768 analysis), and resulted in a smaller area-strike frequency. We estimate that the Calvert Cliffs MIP (or Ψ) was reduced by a factor of 4 or more. The Calvert Cliffs document does not offer details on the computation of the adjustment factor. As stated in the previous paragraph, there is no need of any adjustment factor on the basis of changes to the tornado frequency alone. The MIP is independent of the input tornado frequency. If the only change in the TORMIS code run is the numeric value of the tornado frequency, the derived MIP will not change. Specifically, if runs are executed adopting area-strike or point-strike frequencies, or different characteristic lengths to compute area-strike frequencies, the MIP results will be the same.

The MIP is the number of hits per missile per unit of target area, given a tornado strike to the site. The MIP is independent of the use of an area-strike frequency or a point-strike frequency,

or of any other approach to compute the tornado frequency. TORMIS runs differing solely on the numeric value of the tornado frequency will yield identical MIP values.

As defined in Eq. [7], if MIP^{NP} is a reference MIP, the frequency of failure of a target or component is proposed by the nuclear energy industry to be computed as $f_{ie} = f\ MIP^{NP} \times (\text{number of missiles}) \times (\text{area of target})$. Assuming MIP^{NP}=MIP_i^{NP} for a specific target i (e.g., Target 6 of Plant A in NP-768) then the product of the site-specific tornado frequency and the reference MIP equals

$$f\ MPI_i^{NP} = \frac{f}{f^{NP}} \frac{H_i^{NP}}{A_i^{NP}} \quad [10]$$

The quantity H_i^{NP}/A_i^{NP} is computed from tables in NP-768. The ratio f/f^{NP} is a scaling factor representing the linearity of the missile hit frequency on the tornado frequency. If the site-specific tornado frequency f is twice the reference frequency f^{NP}, and if everything else remains the same, TORMIS must produce twice as many target hits. Eq. [10] properly reflects this linear relationship that can be derived from data in the NP-768 report.

2.2 The Missile Hit Frequency Is Affected by Height of Target and Mutual Target Shielding

This section examines the question

- Does the distribution of buildings in a nuclear power plant, and the geometry and dimensions of those buildings, affect the MIP?

We concluded that the relative location of buildings in a plant and the geometry (mainly the height) affects the MIP. The detailed analysis in support of this conclusion is provided next.

The NP-768 report presented results for seven targets of Plant A. The geometry of Plant A is shown in Figure 2, from top and side perspectives. The dimensions of Plant A buildings are listed in Table 1. Figure 2 is an enhanced rendering of NP-768 Figure 3-1, considering information in NP-768 Table 3-1. Fractions of the faces of buildings are covered by the surrounding buildings. For example, buildings 3 and 4 have three faces and the roofs exposed; the south face of building 2 is partially covered by building 4. The lower wall of building 1, containment building, is protected by buildings 2 and 3; only the upper part of the containment building, including the dome, are exposed. Buildings 5, 6, and 7 are fully exposed; however, buildings 5 and 7 are proximal to the central buildings, and, as demonstrated in the discussion that follows, buildings 5 and 7 are partially protected by the central buildings against tornados. Building 6 is maximally exposed to tornado influence.

NP-768 states that missile hits along the vertical direction on a building are non-uniform (the precise distribution of hits along the vertical direction is not provided in NP-768; see NP-768 Sections 3.2.2.2 and 3.2.3.4). Figure 3 is a schematic of the number of hits on a target wall (south wall of Target 4). The red color means high number of hits and blue color, low number of hits. This figure is not based on an actual computation, but on visual interpretation of Figure 3-3 in NP-768 and the qualitative discussion in NP-768 Sections 3.2.2.2 and 3.2.3.4 (again, the actual data to construct NP-768 Figure 3-3 are not available). In Figure 3, the number of hits enclosed in the rectangle 1 is less than the number of hits enclosed in the rectangle 2. Thus, the hit density (hits/area) for rectangle 1 is less than the hit density for rectangle 2, and this

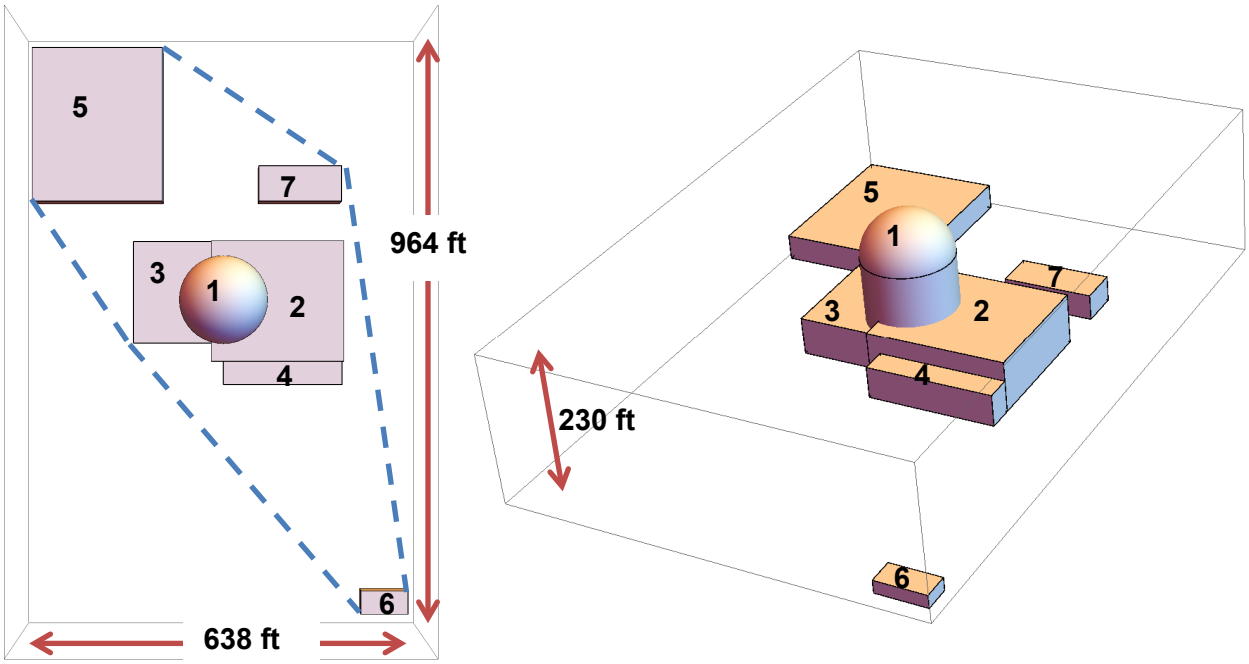

Figure 2. Nuclear Power Plant A, Observed From Top and Side Perspectives. The Dotted Contour Is Referred to as Safety Envelope: a Tornado that Intercepts the Safety Envelope Is Considered to Strike the Facility.

Table 1. Dimensions of Targets for Plant A (Length, Width, and Height Data From NP-768 Table 3-1)

Target Number	Description	Length (ft)	Width (ft)	Height (ft)	Exposed Wall Area (ft^2)	Roof Area (ft^2)	Center X Coordinate (ft)	Center Y Coordinate (ft)
1	Containment	140	Diameter	230	39,584	30,787	2,600	70
2	Auxiliary	220	200	80	44,200	36,303	2,690	70
3	Fuel handling	130	170	60	25,800	14,403	2,515	85
4	Diesel generator	200	40	50	14,000	8,000	2,700	-50
5	Waste processing	220	260	40	38,400	57,200	2,387	370
6	Service water intake	80	40	20	4,800	3,200	2,875	-444
7	Tanks enclosure	140	60	40	16,000	8,400	2,730	270
				Total exposed wall area (ft^2)	182,784.07	158,294	**Total roof area (ft^2)**	
					Total exposed area (ft^2)	341,078		

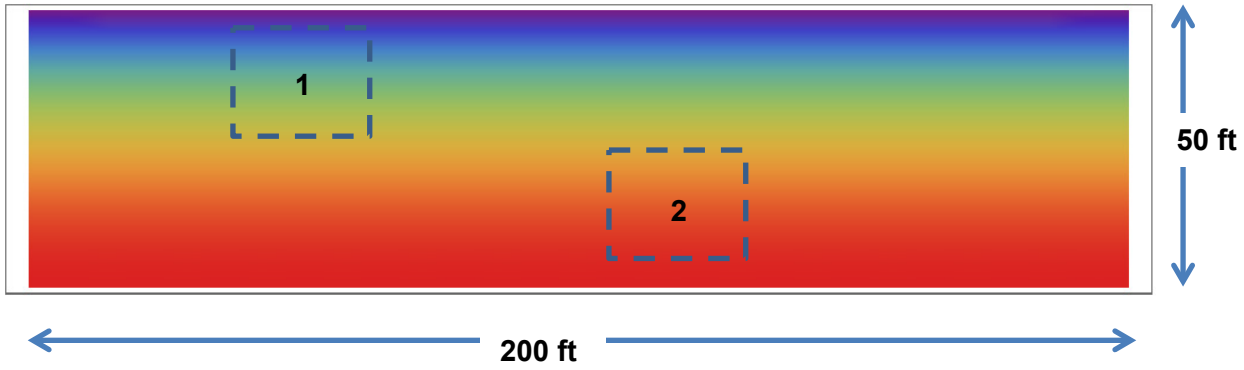

Figure 3. Schematic of the Number of Hits in South Wall of Target 4. Red Color Indicates High Hit Density and Blue, Low Hit Density. This Schematic is Based on Visual Interpretation of Figure 3-3 in NP-768 and Discussions in NP-768, and not on Computations.

implies that MIP(rectangle 1)<MIP(rectangle 2). The MIP computed over the whole 200 ft × 50 ft area is an average MIP for that specific wall, which falls between MIP(rectangle 1) and MIP(rectangle 2). The main point is that the MIP is a quantity that depends on the vertical placement and size of the selected reference area. This fact helps to understand, for example, that the average hit density for shorter buildings (e.g., Targets 4 and 6) is greater than the hit density for taller buildings (e.g., Target 1, containment building).

The Table 2 includes computations of the aggregated MIP per target for tornado intensities in excess of F'2. The sources of the data are indicated in the comment box at the bottom of Table 2. Two different normalizing areas were used to compute the MIP, to account for the observation that missile hits concentrate on the lower parts of buildings (see Figure 3). Roofs would be expected to receive a minor fraction of the missile hits. Based on visual information in NP-768, Figure 3-2 (depicting some missile trajectories for an F'6 tornado), the NP-768 report concludes that "roof impacts are much less likely than wall impacts." To compute the MIP per target (last two columns in Table 2), the total hit frequency per missile (sum of the hit frequency per missile for the tornado intensity brackets) was divided by the mean frequency of a tornado of intensity F'2 or higher (1.36×10^{-3} 1/yr in Table 2, last value in the last row) and a reference area. The reference area was either the exposed wall area or the total exposed area (wall + roof). Magnitudes of these areas are included in Table 2.

Figure 4 is provided to facilitate comparison of the hit frequency and the average MIP for different targets. Figure 4(a) shows the total hit frequency (in units of hits/missile-yr) of the seven targets. The largest targets, Targets 1, 2, and 5, are not the targets with the largest number of hits. Quite the contrary, Target 4, the second smallest target, exhibited the largest number of hits. There is no clear correlation between the size of the exposed surface of the target and the number of hits. Correlations are broken by dependence of the number of hits on the height of the facility and whether there is mutual shielding among the targets. Figure 4(b) displays the MIP using two different reference areas. The circles in Figure 4(b) were computed using the exposed wall area, and the squares employing the total exposed area (wall + roof). The total area MIP is approximately a factor 0.6 smaller than the wall area MIP. As anticipated, the Target 6 yields the highest MIP. As in Figure 2, the Target 6 is the shortest and the most isolated (i.e., Target 6 is the least shielded or protected by the other targets), and thus this

Table 2. Missile Impact Probability per Target, Considering the Exposed Wall and Total Exposed Areas, Plant A

Target No.	Description	Exposed Wall Area (ft^2)*	Roof Area (ft^2)*	Total Exposed Area (ft^2)	Hit Frequency per Missile (hits/missile-yr) per Tornado Intensity Bracket, Region I¥					Total Hit Frequency (Hits/ Missile-yr)	MIP (Exposed Wall) (Hits/ Missile-ft^2)‡	MIP (Total Exposed Area) (hits/ missile-ft^2)‡
					F'2 ≤ Tornado < F'3	F'3 ≤ Tornado < F'4	F'4 ≤ Tornado < F'5	F'5 ≤ Tornado < F'6	Tornado ≥ F'6			
1	Containment	3.96E+4	3.08E+4	7.04E+4	1.52E-10	3.88E-10	1.49E-10	4.27E-11	3.34E-11	7.65E-10	1.42E-11	8.00E-12
2	Auxiliary building	4.42E+4	3.63E+4	8.05E+4	1.11E-09	5.37E-09	1.31E-09	3.53E-09	6.97E-10	1.20E-08	2.00E-10	1.10E-10
3	Fuel handling building	2.58E+4	1.44E+4	4.02E+4	2.44E-09	2.64E-09	1.36E-09	1.91E-09	6.82E-10	9.03E-09	2.58E-10	1.65E-10
4	Diesel generator building	1.40E+4	8.00E+3	2.20E+4	5.13E-09	7.41E-09	2.71E-09	1.57E-09	5.77E-10	1.74E-08	9.14E-10	5.82E-10
5	Waste processing building	3.84E+4	5.72E+4	9.56E+4	4.53E-09	1.34E-09	**1.24E-09†**	2.68E-09	1.32E-09	1.11E-08	2.13E-10	8.55E-11
6	Service water intake structure	4.80E+3	3.20E+3	8.00E+3	1.75E-09	5.45E-09	2.74E-10	4.10E-10	9.68E-11	7.98E-09	1.22E-09	7.34E-10
7	Tanks enclosure	1.60E+4	8.40E+3	2.44E+4	1.12E-09	2.66E-09	1.77E-09	1.30E-09	5.87E-10	7.44E-09	3.42E-10	2.24E-10
			Region I Tornado Frequency Brackets ₹		**F'2 ≤ tornado < F'3 (1/yr)**	**F'3 ≤ tornado < F'4 (1/yr)**	**F'4 ≤ tornado < F'5 (1/yr)**	**F'5 ≤ tornado < F'6 (1/yr)**	**Tornado ≥ F'6 (1/yr)**	**Tornado intensity ≥ F'2 (1/yr)**		
					8.17E-4	3.77E-4	1.18E-4	3.86E-5	8.78E-6	**1.36E-3‡**		

* The exposed wall and roof area are from Table 1 in this report.
¥ Source of hit frequency per missile per target per F' intensity bracket is NP-768 tables 3-8 to 3-14, column for H (hit frequency), Region I
† The source NP-768 Table 3-12 indicates this value to be 1.24×10^{-8} 1/missile-yr, due to a typographical error. The correct value is 1.24×10^{-9} 1/missile-yr
₹ The Source of the tornado frequency brackets is NP-768 Table 3-4, mean values, Region I frequencies
‡ The frequency for a tornado to exceed the F'2 intensity (0.00136 1/yr) was used to compute the missile impact probability (MIP)

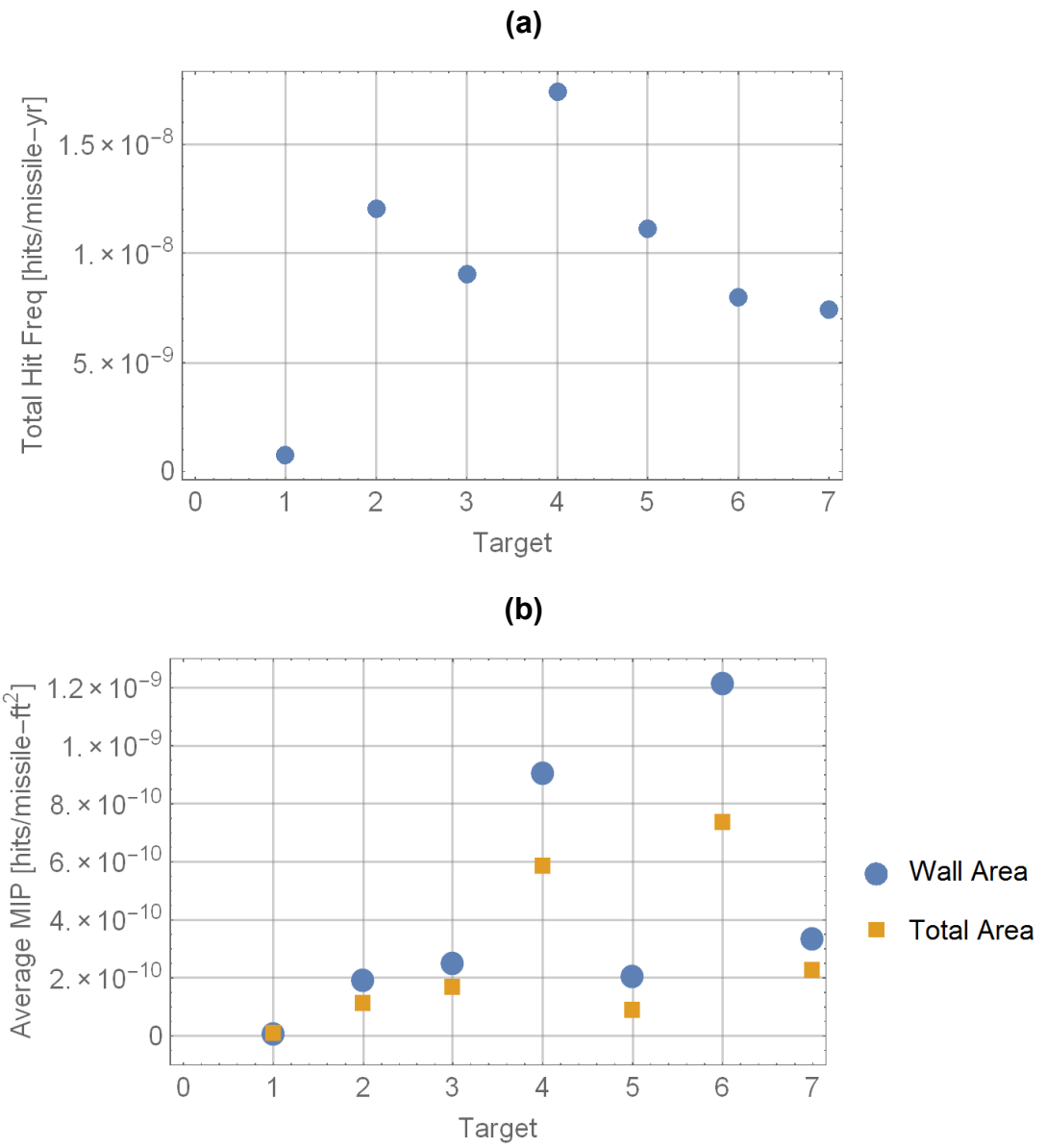

Figure 4. (a) Total Missile Hit Frequency (in Units of Hits/Missile-yr) and (b) Average MIP for the Different Targets. In Computing the MIP, Two Normalization Areas Were Considered: Exposed Wall Area and Total Area (Exposed Wall Area + Roof). The Two Alternative MIP Values per Target Are Displayed in (b). Consult Table 2 for Data Sources.

combination of features of Target 6 causes its MIP to be the highest. By contrast, Target 1 is the containment building and it is the tallest. It is well protected in the lower wall by the other targets, resulting in the lowest MIP. The next target with the highest MIP is Target 4. From Figure 2, the dominant exposed area is the south wall, which is unprotected by other targets. Target 4 is taller than Target 6, and this causes the MIP for Target 4 to be smaller than the MIP for Target 6. If Target 4 was of similar height as Target 6, we conjecture that the MIP for these targets would be similar. Targets 5 and 7 are of the same height. These two targets appear similarly shielded by other targets in the system; however, the MIP for Target 7 is greater than the MIP for Target 5. Targets 2, 3, and 5 yield comparable MIPs, despite contrast in heights

and mutual target shielding. The main point of this assessment is that the dependence of MIP on target height and mutual target shielding makes it difficult to predict the scale of the MIP value except in simple cases, such as Target 6 (shortest target and most isolated) and Target 1 (tallest target and most protected), which have the highest and lowest MIP values.

2.3 The MIP Is a Function of the Tornado Intensity

This section examines whether or not the MIP is a function of the tornado intensity. As the title of the section implies, we concluded that the MIP is indeed a function of the tornado intensity. Higher wind speeds cause longer missile paths, which increase the likelihood that a missile will hit a target. Accordingly, the MIP is expected to increase with increasing tornado intensity. Figure 5 details the approach to compute the MIP from data in Table 2, for each of the targets. The plot in Figure 5(a) is the hit frequency (in units of hits/missile-yr) for Region I from Table 2 (the original data are from NP-768 Tables 3-8 to 3-14). The decreasing trend of the curves is due to the decreasing frequency of the higher tornado intensities. Figure 5(b) is the hit frequency from Figure 5(a) divided by the tornado intensity frequency bracket (last row in Table 2). The resulting trend is increasing, consistent with the observation that tornados of higher intensity are expected to produce relatively more missile hits (due to longer missile trajectories). The data for Figure 5(b) correspond to Region I; however, as previously argued, the ratio of the hit frequency to the tornado frequency is independent of the tornado region (see Figure 6). The last step to compute the MIP is normalizing data in Figure 5(b) by the target area. The MIP in Figures 5(c) and (d) was computed by dividing the data from Figure 5(b) by the exposed wall area and the total exposed area, respectively (3^{rd} and 5^{th} columns in Table 2). The resulting MIP is predominantly an increasing function of the tornado intensity. In consistency with results in the previous section, Figure 5(d) shows that the MIP values for Targets 4 and 6 are the highest, and the MIP for Target 1 is the lowest.

Figure 6 is included to reinforce the conclusion that the MIP is independent of the NRC tornado region. Using Region II and III data (data not tabulated in this report, for brevity), following the approach defined in the previous paragraph, the corresponding MIP for those regions was computed. The MIP(Regions I) is identical to MIP(Region II), except at F'5 tornado intensity. The MIP(Region II) is identical to MIP(Region III), except at F'4 intensity. These differences at higher F' tornado intensities are likely due to statistical artifacts.

An anomalous MIP local maximum for Target 2 occurs at F'3 [see Figures 5(c), (d) and 6]. It is not clear whether this local spike has a physical reason or it is due to a numerical artifact. It is possible that the F'3 spike may be due to statistical convergence issues, in which case the spike would disappear when larger statistical samples (i.e., more tornado events, more missiles, and more statistical realizations) are considered. The presence of spikes and sharp inflections in Figures 5 and 6 suggests lack of statistical convergence.

In conclusion, the MIP is an increasing function of the F' tornado intensity. The MIP is independent of the tornado region. Using data reported in NP-768, inflections and spikes in MIP versus F' tornado scale are observed, which may be indicative of lack of statistical convergence in the computation of the MIP. However, this potential lack of statistical convergence is less relevant than other factors noted in this report affecting the magnitude of the MIP (e.g., mutual shielding or targets and dependence of the MIP on the target height).

(a)

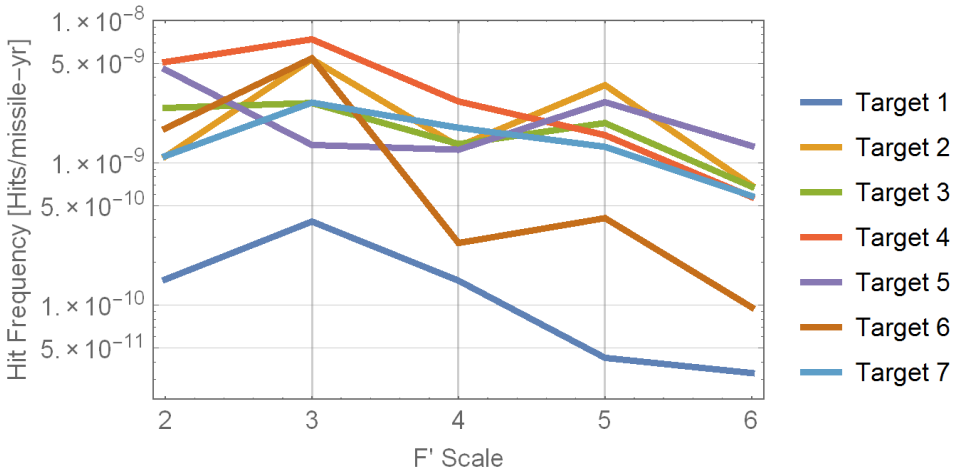

(b)

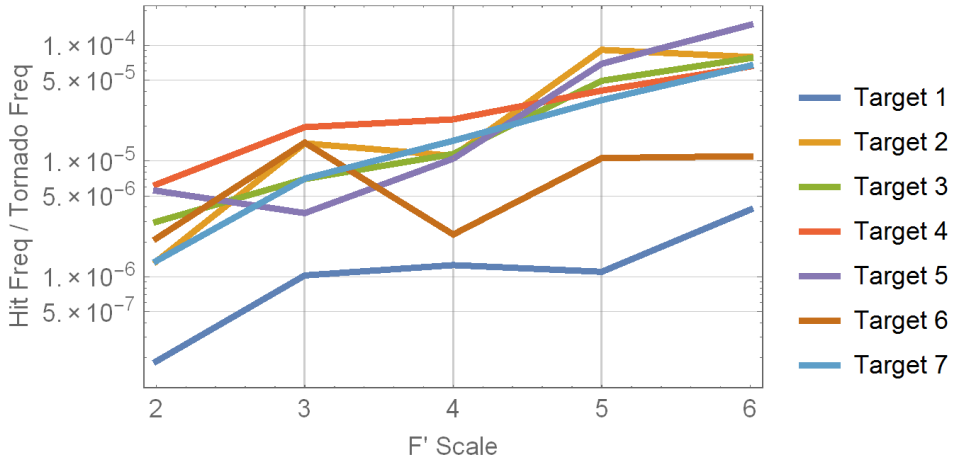

Figure 5. (a) Hit Frequency per Missile Versus F' Scale (Data from Table 2). (b) Data from Plot (a) Divided by the F' Tornado Intensity Frequency (Last Row in Table 2).

(c)

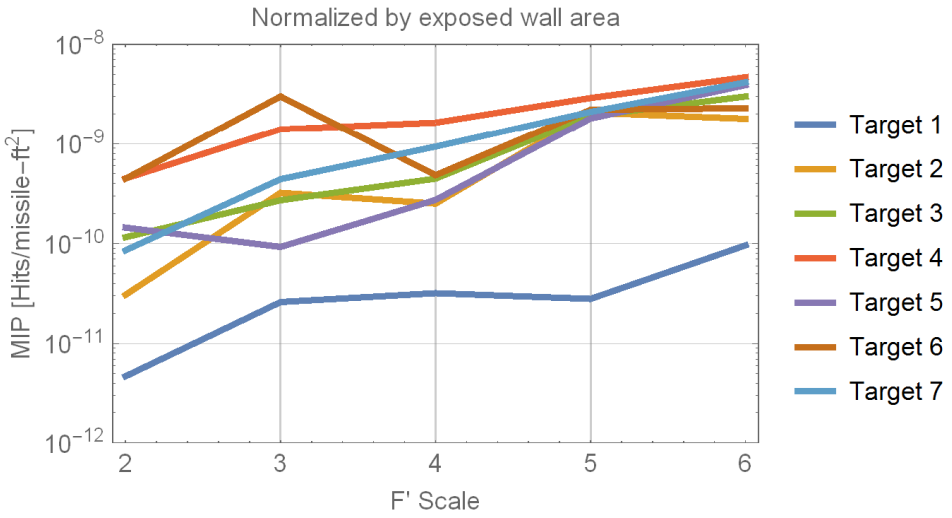

(d)

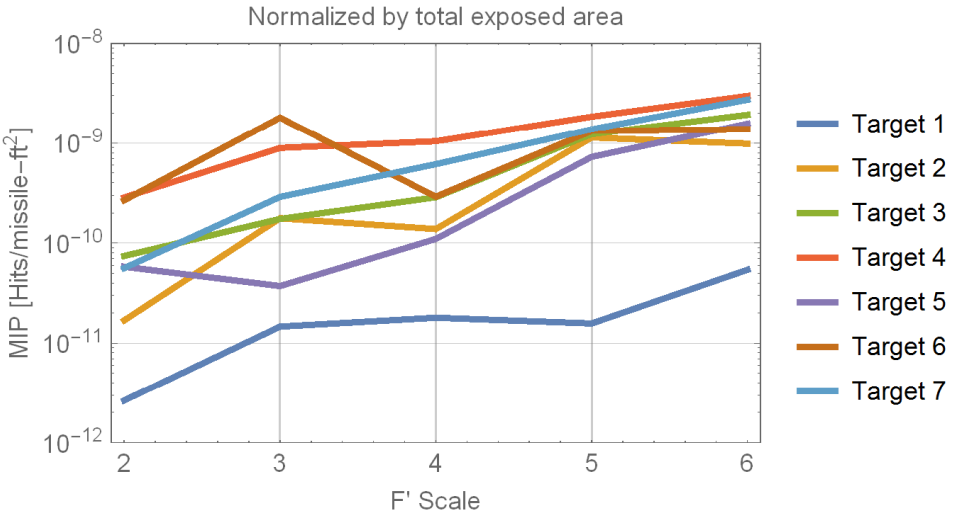

Figure 5 (Continued). (c) Exposed Wall MIP: Data From Plot (b) Divided by the Exposed Wall Area (3rd Column in Table 2). (d) Total Area MIP: Data From Plot (b) Divided by the Total Exposed Area (5th Column in Table 2).

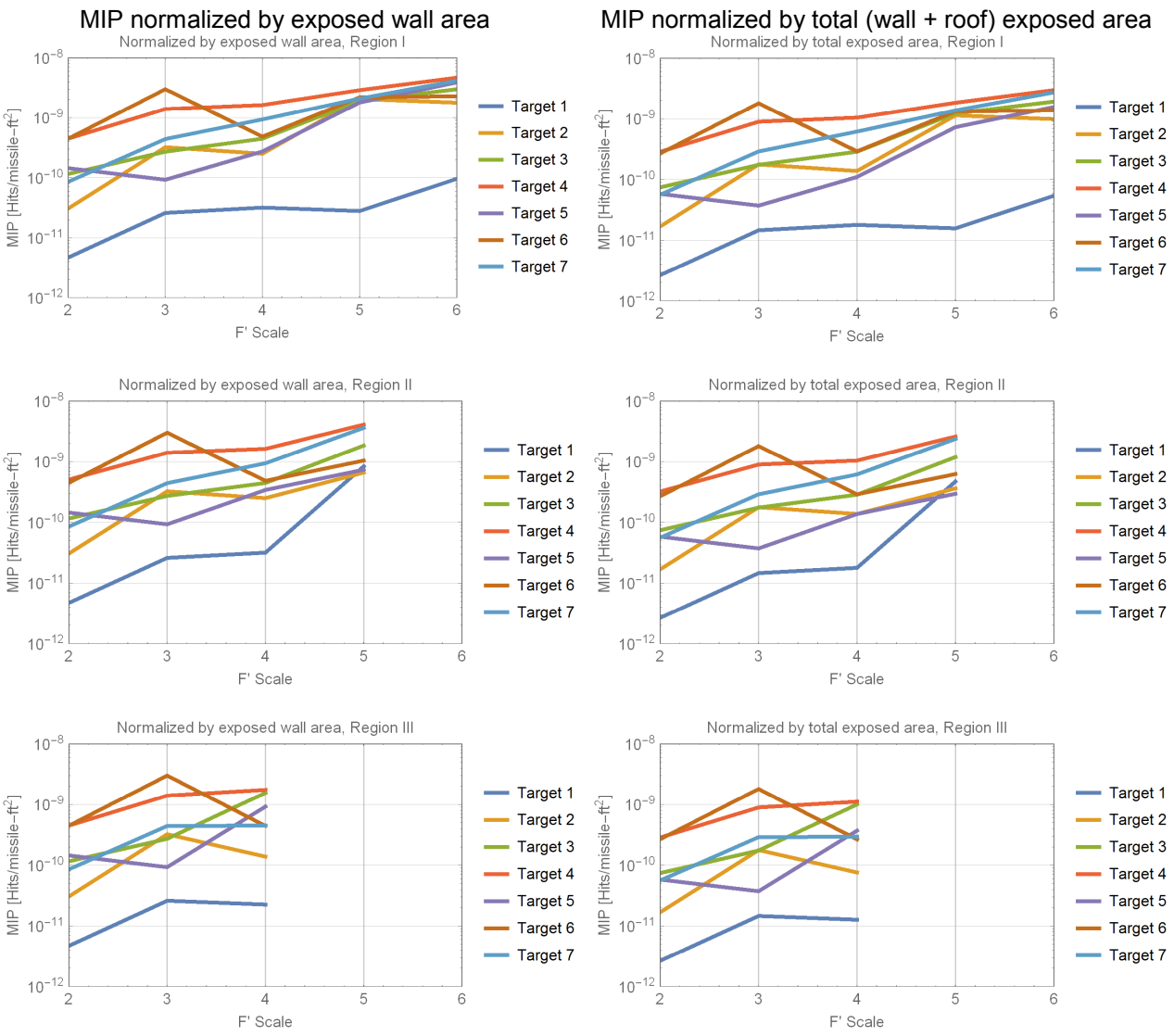

Figure 6. MIP Computed with Region I, II, and III Data. The Results Are Nearly Identical, with Differences Only at High F' Intensity, Possibly Due to Statistical Artifacts. Hit Frequencies Were Obtained From NP-768 Tables 3-8 to 3-14. Tornado Frequency Data for the Three Regions Come From NP-768 Table 3-4. The Exposed Area of the Seven Targets Is Listed in Tables 1 and 2 of this Report.

2.4 The MIP Is a Function of the Initial Missile Spread

This section examines the question

- What is the relationship of features of missiles (e.g., initial location and initial insertion height) to the MIP and the scaling approach (Eq. [7])?

We found that the extent of the initial missile spread is an essential aspect of the NP-768 analysis, and that if the spread at a site is different than in the conditions of the hypothetical Plant A, then care should be exercised in the linear scaling approach. The number of hits and the hit frequency do not necessarily linearly scale with the number of missiles, if the missiles are not initially distributed as in the Plant A configuration. Conservative correction factors on the MIP can be designed to preserve the linear scaling approach. The analysis supporting this conclusion and details on possible MIP correction factors are provided as follows.

The missiles in the analysis of Plant A in NP-768 are initially spread over a broad area (a rectangle of dimensions 4,640 ft × 5,000 ft). In this section we analyzed the effect of a different area of spread on estimates on the number of hits on a target. Section 3.2.3.4 of NP-768 states that out of 48 high-speed impacts recorded in NP-768, Figure 3-2, only two missiles traveled more than 425 feet. One was a utility pole that traveled 720 feet. NP-768, Figure 3-2, is interpreted by the authors of that report to indicate that the length of the trajectory of the majority of high-speed missiles hitting a target is less than 300 feet. A corollary of this statement is that the majority of the missiles (high speed and low speed) would travel less than 300 feet. A document prepared by Calvert Cliffs NPP (1994) analyzed appendices to the NP-768 report and concluded that the mean displacement range of missiles in the NP-768 study was less than 350 feet, and that no missiles traveled more than 2,000 feet. Calver Cliffs NPP concluded that strikes were dominated by “close-in missiles.”

Figure 7 is a qualitative schematic of the distribution of the initial position of missiles hitting a target in Plant A. The schematic is not based on computations, but on interpretations of descriptions provided in the NP-768 Section 3.2.3.4 and the Calvert Cliffs NPP (1994) documents (i.e., data are not available in NP-768 on the initial location of missiles hitting targets). Figure 7 conveys the point that the majority of the missiles that hit a target originate near to the Plant A (in the regions of hot or warm colors in Figure 7), and that missiles starting distant to the Plant A (in regions of cool colors in Figure 7) are unlikely to hit any target.

From Eqs. [6] and [9],

$$\frac{H_i^{NP}}{f^{NP}} = A_i^{NP}\, MIP_i^{NP} = \frac{h_i^{NP}}{M_s} \qquad [11]$$

f^{NP} – tornado frequency
h_i^{NP} – number of hits on target i
M_s – total number of missiles in the NP-768 simulations

In the NP-768 analysis, the M_s missiles are considered not to interact among them (no cross-hits and bounces between missiles). This assumption causes the ratio h_i^{NP}/M_s to be independent of the number of missiles. In other words, if the number of missiles doubles or triples, the number of hits would double or triple as well. Again, this linear proportionality

between h_i^{NP} and M_s arises from the assumed independence of the missiles. Because of this proportionality,

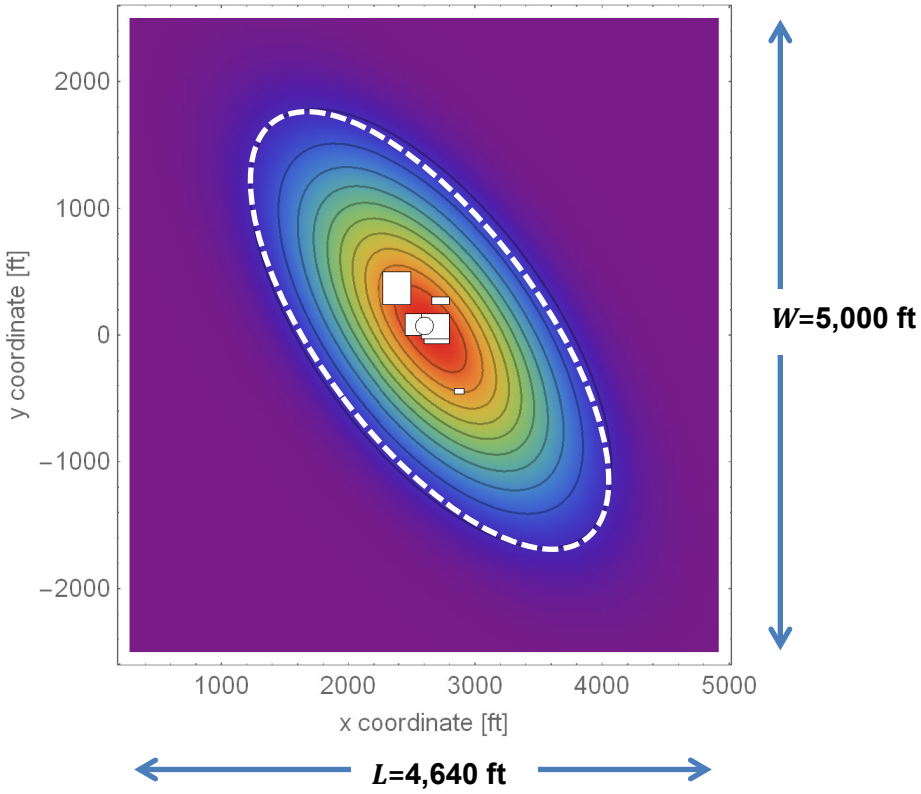

Figure 7. Qualitative Distribution of Initial Missile Locales Causing Target Hits. The Majority of the Hitting Missiles Originate in Warm Color Areas (Close to the Plant), and Few Hitting Missiles Start in Cool Color Regions (Far from the Plant). The Distribution Plot Is Not Based on Computations, but on Interpretation of Discussions in NP-768. The White Structure in the Center of the Graphic Is the Top View of Plant A.

the MIP is independent of the number of missiles M_s considered in the NP-768 analysis, provided M_s is large enough to ensure statistical convergence.

From Eq. [11], the quantity

$$h = MIP^{NP} \times (\text{number of missiles}) \times (\text{area of target}) \qquad [12]$$

is an estimate of the number of hits, h, on a target, given a tornado strike. In the NP-768 analysis, the total number of missiles, M_s, are assumed uniformly spread over the whole 4,640 ft × 5,000 ft area enclosing Plant A. This assumption is of outmost importance. If this assumption is false (for example if the missile spread is not uniform, or the spread is over an area different than 4,640 ft × 5,000 ft, then the estimate of the number of hits by Eq. [12] is not only inaccurate but potentially non-conservative. An example is presented to clarify this statement.

The uniform missile density (number of missiles per unit of area) is defined as

$$\rho_m^{NP} = \frac{M_S}{L\,W} \quad [13]$$

L and W are length and width of the area of analysis (L = 4,640 ft and W = 5,000 ft in the NP-768 analysis, see Figure 7). The missiles enclosed in the dotted-line oval in Figure 7 are the majority of that could hit targets. Thus, if a TORMIS analysis was performed considering only the missiles enclosed in that oval, the computed number of hits on target *i* would be nearly identical to the number of hits considering missiles spread over the complete $L \times W$ area, h_i.

To illustrate this effect, assume the number of missiles during an actual survey are fully enclosed inside the dotted line oval in Figure 7. For simplicity (but without loss of generality), assume the missile density of the survey is uniform and equal to ρ_m^{NP} (Eq. [13]). Thus, the missile count, M, would be

$$M = \rho_m^{NP} S_{oval} = M_s \frac{S_{oval}}{L\,W} \quad [14]$$

S_{oval} is the area enclosed by the dotted-line oval in Figure 7. The number of missile hits on target *i* estimated using Eq. [12] (the proposed industry approach) would be

$$h_i = MIP_i^{NP}\ M\ A_i^{NP} = M_s\, A_i^{NP}\, MIP_i^{NP} \frac{S_{oval}}{L\,W} = h_i^{NP} \frac{S_{oval}}{L\,W} < h_i^{NP} \quad [15]$$

Therefore, the estimated number of hits using the scaling industry approach, h_i, is less than the number of hits h_i^{NP} that would be derived using a detailed TORMIS run (again, a detailed TORMIS run would output a number close to h_i^{NP}, because the dotted line oval encloses almost all of the hitting missiles). Based on this simple analysis, we conclude that the scaling approach proposed by the nuclear energy industry underestimates the number of missile hits.

Re-Scaling the MIP to Avoid Underestimating the Number of Missile Hits

If the survey missiles are uniformly spread over an area S, then the following adjustment may be adopted to avoid undercounting the number of missile hits:

$$\overline{MIP_i} = MIP_i^{NP}\ \frac{L\,W}{S} \quad [16]$$

The factor $L\,W/S$ can be significantly greater than one, if the area of missile spread S is small compared to the NP-768 $L\,W$ area. With this correction, analyzing the example where the missiles are enclosed in the dotted-line oval in Figure 7, and assuming M is the number of missiles enclosed in the oval and S=S_{oval}, the number of missile hits on target i (of area A_i^{NP}) would be estimated as

$$h_i = M\,\overline{MIP_i}\,A_i^{NP} = M\,A_i^{NP}\,MIP_i^{NP}\ \frac{L\,W}{S_{oval}} = \frac{M}{S_{oval}}\,\frac{L\,W}{M_s}\,h_i^{NP} \quad [17]$$

If the missile density, ρ_m=M/S_{oval}, is the same as the NP-768 missile density, $\rho_m^{NP} = M_s/(L\,W)$, then $h_i = h_i^{NP}$ (i.e., the same number of hits as computed in NP-768 is recovered). Equation [16] can be rewritten as

$$\overline{MIP_i} = MIP_i^{NP} \ \frac{\rho_m}{\rho_{average}} \qquad [18]$$

where $\rho_{average}$ is the total number of missiles divided by the constant $L\,W$ (= 2.32 × 10^7 ft^2) area, and the missile density, ρ_m, is the number of missiles divided by the actual initial spread area, S. With this correction, the number of missile hits on a target would be computed as

$$h = \frac{\rho_m}{\rho_{average}} MIP^{NP} \times (\text{number of missiles}) \times (\text{area of target}) \qquad [19]$$

This equation is a correction to Eq. [12] that the nuclear energy industry proposes to compute the number of missile hits. Equation [12] does not explicitly recognize that missiles in the NP-768 analysis are fully spread over a fixed area $L\,W$. If the missile spread is different, then Eq. [12] can underestimate the number of missile hits, as demonstrated in the Figure 7 example.

A natural question is how to re-scale the MIP in case of non-uniform missile distributions. For example, Figure 8(a) includes two clusters of missiles spread over an oval and a triangle. The number of missiles and area of the missile cluster are M_1 and S_1 for the oval, and M_2 and S_2 for the triangle. The missile densities ρ_{m1}=M_1/S_1 and ρ_{m2}=M_2/S_2 may be different (the distribution of missiles is non-uniform in the L×W area, but uniform within the oval and the triangle). In similitude to Eq. [16], the proposed adjustment to the MIP is

$$\overline{MIP_i} = MIP_i^{NP} \ \frac{L\,W}{S_1 + S_2} = MIP_i^{NP} \ \frac{\bar{\rho}_m}{\rho_{average}} \qquad [20]$$

The term $\bar{\rho}_m$= $(M_1$+$M_2)/(S_1$+$S_2)$ is the average missile cluster density of the problem in Figure 8(a). The term $\rho_{average}$ is computed as $\rho_{average} = (M_1 + M_2)/(L\,W)$. The number of hits with the corrected MIP, $\overline{MIP_i}$, for target i (of area A_i^{NP}) would be estimated as

$$h_i = (M_1 + M_2)\,\overline{MIP_i}\,A_i^{NP} = \frac{M_1 + M_2}{S_1 + S_2} \ \frac{h_i^{NP}}{\rho_m^{NP}} = \frac{\bar{\rho}_m}{\rho_m^{NP}} \ h_i^{NP} \qquad [21]$$

The proposed MIP correction ignores the distance of the missile cluster to the target, which is a conservative approach. For example, consider the case where M_2=0 (i.e., all of the missiles are in the oval). In that case, Eq. [21] becomes identical to Eq. [17]. If the missile density ρ_{m1}=M_1/S_1 was identical to ρ_m^{NP}, the estimated number of hits for target i, h_i, would equal h_i^{NP}. The oval in Figure 8(a) is distant to the targets, at a location where few or no missiles would be expected to hit any target. A detailed TORMIS run would produce a very small number of hits or no hits from missiles in the oval. Clearly, the estimated number of hits using the scaling approach is conservative in this example. To propose a more accurate adjustment to the MIP, the distance of the missile cluster to the target has to be accounted for and additional TORMIS runs are needed. Absent such information, the conservative correction in Eq, [20] is reasonable.

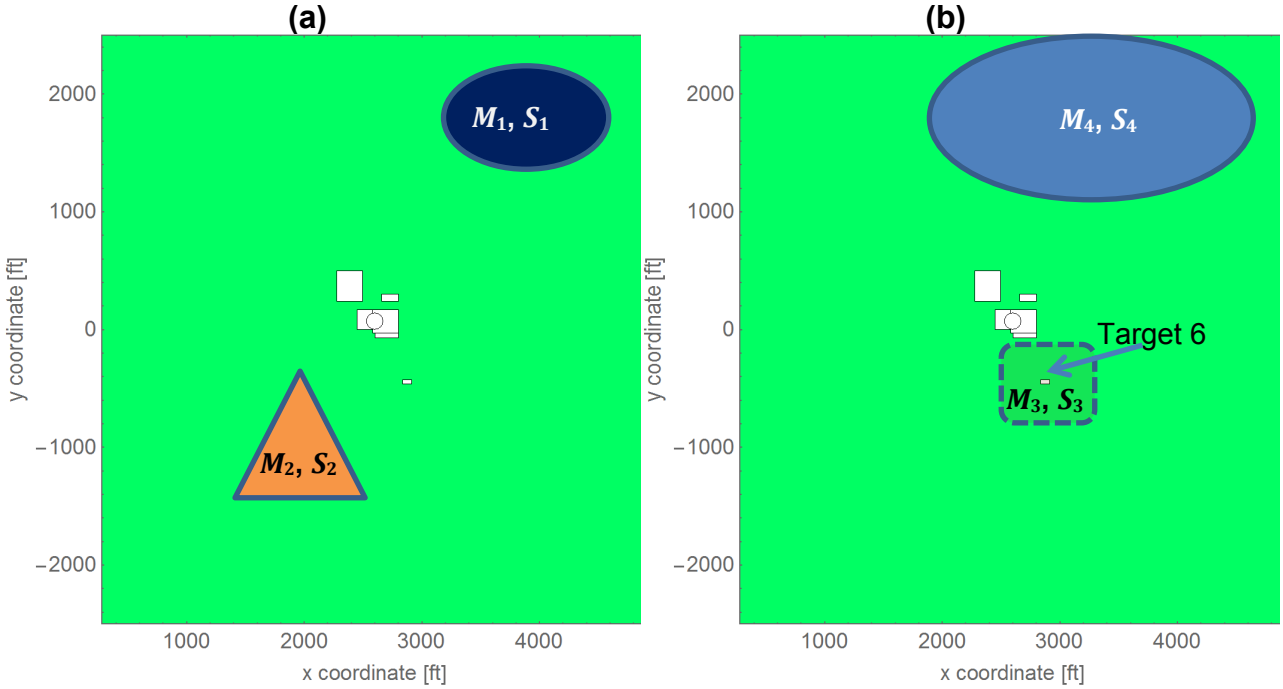

Figure 8. Plant A with Two Clusters of Missiles. The symbols M_i and S_i Represent the Number of Missiles and their Spread Area, Respectively.

The correction in Eq. [20] may be generalized for multiple missile clusters:

$$\overline{MIP_i} = MIP_i^{NP}\, L\, W \left(\sum_{j=1}^{n_c} S_j \right)^{-1} = MIP_i^{NP}\, \frac{\bar{\rho}_m}{\rho_{average}} \qquad [22]$$

$\bar{\rho}_m$ is the average missile cluster density:

$$\bar{\rho}_m = \frac{\sum_{j=1}^{n_c} M_j}{\sum_{j=1}^{n_c} S_i} \qquad [23]$$

Equation [29] remains valid, replacing ρ_m by $\bar{\rho}_m$:

$$h = \frac{\bar{\rho}_m}{\rho_{average}} MIP^{NP} \times (\text{number of missiles}) \times (\text{area of target}) \qquad [24]$$

Care needs to be exercised in using an average missile cluster density, as it can also lead to underestimating the number of missile hits. Figure 8(b) is provided to explain this possibility. The dotted-line rectangle is surrounding Target 6. Clearly, the relevant missile density to

compute the number of hits is $\rho_{m3}=M_3/S_3$, which is the density surrounding Target 6. The number of hits on Target 6 should be dominated by the nearby missiles. The number of hits, in this case, should be estimated as $MIP_i^{NP768}(\rho_{m3}\ L\ W) \times (\text{area of Target } 6)$.

Equation [24] calls for the use of the average missile density, $\bar{\rho}_m$, to compute the number of missile hits. If the number of missiles in the oval, M_4 is small, then the average cluster density $\bar{\rho}_m$ (see Eq. [23]) can be significantly smaller than the local density, ρ_{m3}. The number of missile hits using Eq. [24] for the problem in Figure 8(b) can be greatly underestimated. Thus, judgement should be applied in using Eq. [24]. The average missile density $\bar{\rho}_m$ may be replaced instead by the density of the missile cluster closest to the target or by the largest missile density.

In summary, the nuclear energy industry is implicitly proposing estimating the number of hits on a target, given a tornado strike, as $MIP^{NP} \times (\text{number of missiles}) \times (\text{area of target})$. An example was provided (see Figure 7 and related text) to demonstrate that this approach may underestimate the number of hits on a target. The reason is that the number of hits does not scale linearly with the number of missiles. The number of hits depends on the distance to the target and the missile spread. A reasonable approach to computing the number of hits is

$$h = \frac{\bar{\rho}_m}{\rho_{average}} MIP^{NP} \times (\text{number of missiles}) \times (\text{area of target}) = MIP^{NP}(\bar{\rho}_m\ L\ W) \times (\text{area of target}) \quad [25]$$

The quantity $\bar{\rho}_m\ L\ W$ is an equivalent number of missiles, $L\ W$ is the area of the NP-768 analysis equal to 2.32×10^7 ft^2 (L = 4,640 ft, W = 5,000 ft), and $\rho_{average}$= (number of missiles)/(2.32×10^7 ft^2). The reference missile cluster density $\bar{\rho}_m$ is

$$\bar{\rho}_m = \begin{cases} \dfrac{\sum_{j=1}^{n_c} M_j}{\sum_{j=1}^{n_c} S_i}, \text{ or} \\ \text{Average density of missile clusters closest to target, or} \\ \text{Highest missile cluster density} \end{cases} \quad [26]$$

The analyst needs to apply judgement to select a defensible value of $\bar{\rho}_m$ (in the next section analyzing Plant B, the numerical evidence favors the definition of $\bar{\rho}_m$ as average nearby missile cluster density). In similitude to Eq. [7], the frequency of the initiating event, f_{ie}, would be computed as

$$f_{ie} = f\ \frac{\bar{\rho}_m}{\rho_{average}}\ MIP^{NP} \times (\text{number of missiles}) \times (\text{area of target}) \quad [27]$$

The approach is only slightly different than the approach proposed by the nuclear energy industry, which requires a survey to count the number of missiles. Instead, Eq. [27] calls for identifying the number of missiles, the area of the initial missile spread, and identification of the relevant missile density based on the distance of the missiles to the target. If different clusters of missiles are of comparable density, use of an average missile density is reasonable. If there is high contrast between the different missile densities, the analyst needs to identify a defensible missile density to use in Eq. [27]. The NP-768 Plant B analysis in the next section indicates that it is reasonable to consider the nearby missile cluster density to define $\bar{\rho}_m$.

2.5 Analysis of NP-768 Plant B Configurations

This section continues examining the question

- What is the relationship of features of missiles (e.g., initial location and initial insertion height) to the MIP and the scaling approach (Eq. [7])?

The adjustment to the MIP expressed as Eq. [20] is used to rationalize MIP values computed for the Plant B configurations. Plant B is a 2-unit power plant. Table 3 includes the dimensions of the 16 buildings of Plant B. In the B1 configuration, it is assumed that the second unit is undergoing construction. Buildings 10 to 16 are part of the unit under construction. Accordingly, in the NP-768 analysis, those buildings are considered absent, but the construction material may be a source of missiles. In the B2 configuration, the two units are operational. Figure 9 shows top and side perspectives of the Plant B. Figure 9 is an enhanced rendering of NP-768 Figure 3-4, considering information in NP-768 Table 3-18.

The main difference with respect to the Plant A analysis is the initial non-uniform distribution of missiles. The non-uniformity refers to three different aspects: the number of missiles, the type of missiles, and insertion heights. In the Plant A analysis it was assumed that the missile starting point could be anywhere within the $L\ W$ area, for any of the six types of missiles considered in the analysis. The insertion height in Plant A was 5 to 50 feet for most of the

Table 3. Dimensions of Targets for Plant B (Length, Width, and Height Data From NP-768 Table 3-18)

Target	Description	Length (ft)	Width (ft)	Height (ft)	Exposed Wall Area (ft^2)	Roof Area (ft^2)	Center x Coordinate (ft)	Center y Coordinate (ft)
1	Containment 1	140	Diameter	230	39,584.	30,788	2,597	70
2	Auxiliary Building	220	200	80	34,400	36,303	2,707	70
3	Fuel Handing Building	130	170	60	25,800	14,403	2,532	85
4	Diesel Generator Building	200	40	50	14,000	8,000	2,717	-50
5	Waste Processing Building	220	260	40	38,400	57,200	2,390	370
6	Service Water Intake Structure 1-1	40	40	20	1,600	1,600	2,854	-446
7	Tanks Enclosure	140	60	40	16,000	8,400	2,747	270
8	Service Water Intake Structure 1-2	40	40	20	1,600	1,600	2,894	-446
9	Turbine Building	300	140	70	51,800	42,000	2,967	70
10	Containment 2	140	Diameter	230	39,584	30,788	2,200	70
11	Auxiliary Building 2	200	220	80	34,400	36,303	2,200	-40
12	Fuel Handing Building 2	170	130	60	25,800	14,403	2,185	135
13	Diesel Generator Building 2	40	200	50	14,000	8,000	2,320	-50
14	Tanks Enclosure 2	60	140	40	16,000	8,400	1,927	-80
15	Turbine Building 2	140	300	70	51,800	42,000	2,200	-300
16	Service Water Intake Str. 2	80	40	20	4,000	3,200	2,794	-446

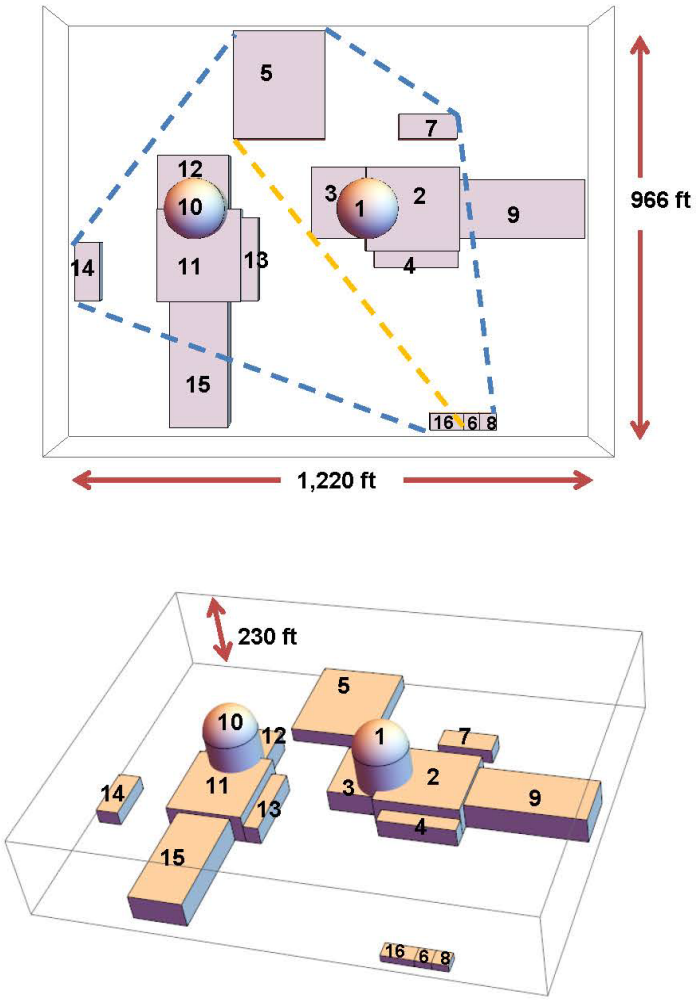

Figure 9. Nuclear Power Plant B, Observed From Top and Side Perspectives. The Blue Dotted Line Contour Is the Safety Envelope of the Whole Plant. The Region Between the Yellow Dotted Line and the Dotted Lines on the Right Side Is the Safety Envelope of the First Unit.

missiles, except for automobiles, which were assumed to be between 5 and 10 feet. On the other hand, in the Plant B configurations, different missile types are distributed differently in missile zones. For example, automobiles are predominantly located in a specific zone (zone 4, parking lot, see Tables 3 and 4). Missiles are inserted at different heights in different zones, as high as 100 ft (in zone 2 in the B1 configuration).

Tables 4 and 5 list the missile distribution among different zones for the B1 and B2 configurations, and the zone missile density (number of missiles/area of zone). The relative missile density ($\rho_m/\rho_{average}$) is shown in the last column. Relative densities close to unity indicate zones that may be directly comparable to the Plant A analysis in NP-768 (taking into account missile type differences and insertion heights). Figure 10 facilitates visualization of the initial

Table 4. Missile Zones for the Plant B1 Configuration

Zone	Description	Length (ft)	Width (ft)	Center x (ft)	Center y (ft)	Area (ft^2)	No. Missiles	ρ_m Missile density (missiles/ft^2)	$\rho_m/\rho_{average}$ Missile density/Average density
1	Unit 1	837	590	2,698.5	205	493,830	150	3.04E-04	1.41
2	Unit 2 construction	200	665	2,180	-122.5	133,000	300	2.26E-03	10.47
3	Area clearing	2,640	365	3,600	-272.5	963,600	150	1.56E-04	0.72
4	Switchyard and area clearing	2,840	2,045	3,500	-1,477.5	5,807,800	500	8.61E-05	0.40
5	Construction and storage	1,800	2,710	1,180	-1,145	4,878,000	3,000	6.15E-04	2.85
6	Storage and parking	2,000	2,290	1,280	1,355	4,580,000	600	1.31E-04	0.61
7	Area clearing	2,640	470	3,600	735	1,240,800	150	1.21E-04	0.56
8	Area clearing	1,803	590	4,018.5	205	1,063,770	150	1.41E-04	0.65
9	Service water discharge basin	2,640	1,530	3,600	1,735	4,039,200	0	0	0

Approximated dimensions were obtained by digitizing NP-768 Figure 3-5(a).
The average missile density, $\rho_{average}$, is computed as 5,000 missiles/2.32×10^7 ft^2 $= 2.16 \times 10^{-4}$ missiles/ft^2.

Table 5. Missile Zones for the Plant B2 Configuration

Zone	Description	Length (ft)	Width (ft)	Center x (ft)	Center y (ft)	Area (ft^2)	No. Missiles	ρ_m Missile density (missiles/ft^2)	$\rho_m/\rho_{average}$ Missile density/Average density
1	Units 1 and 2	1,017	950	2,608.5	25	966,150	100	1.04E-04	2.40
2	Area clearing and permanent storage	1,820	3,000	1,190	-1,000	5,460,000	400	7.33E-05	1.70
3	Switchyard and area clearing	2,820	2,050	3510	-1,475	5,781,000	150	2.59E-05	0.60
4	Plant parking	2,180	2,000	1,370	1,500	4,360,000	100	2.29E-05	0.53
5	Area clearing	1,803	950	4,018.5	25	1,712,850	125	7.30E-05	1.69
6	Area clearing	2,460	500	3,690	750	1,230,000	125	1.02E-04	2.36
7	Service water discharge basin	2,460	1,500	3,690	1,750	3,690,000	0	0	0

Approximated dimensions were obtained by digitizing NP-768 Figure 3-5(b).
The average missile density, $\rho_{average}$, is computed as 1,000 missiles/2.32×10^7 ft^2 $= 4.31 \times 10^{-5}$ missiles/ft^2.

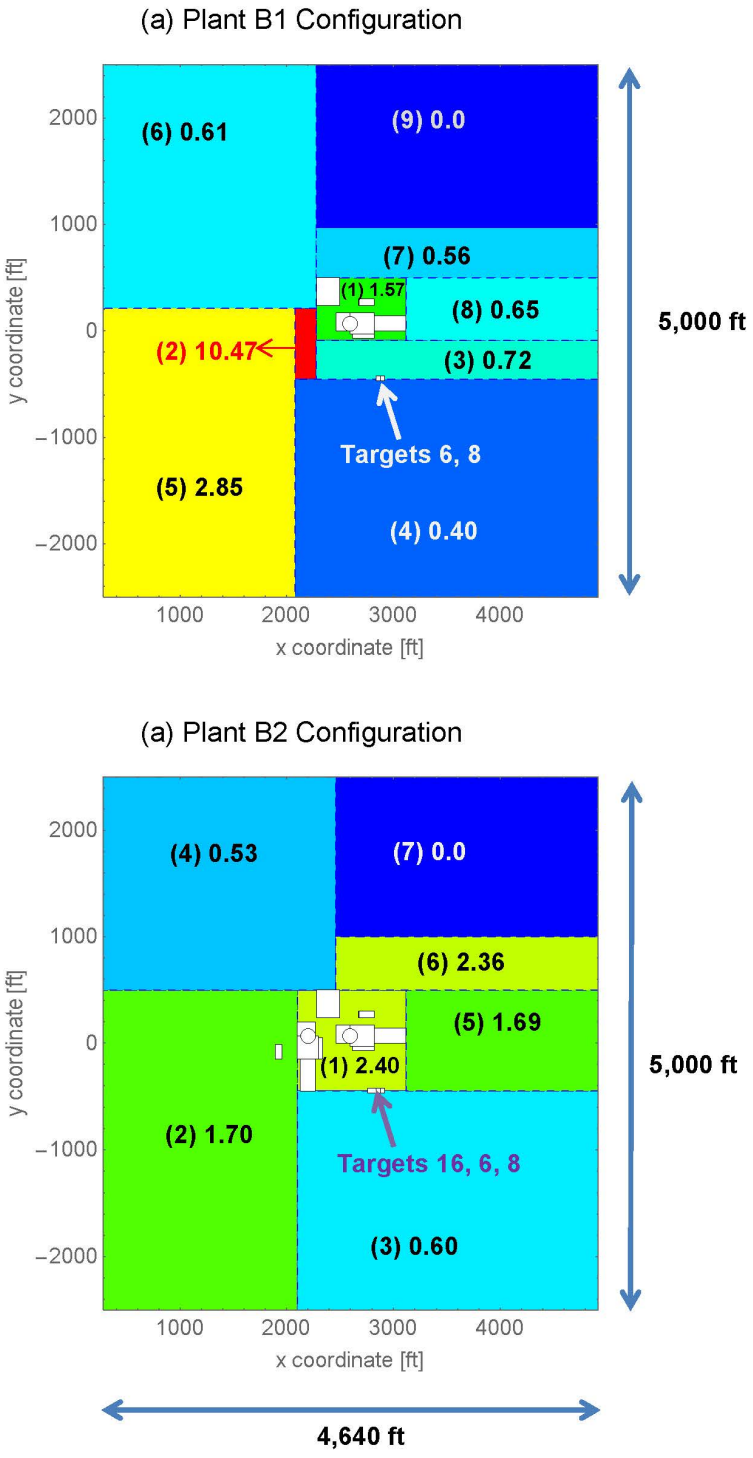

Figure 10. Missile Density for Plant B in B1 Configuration (Unit 2 Under Construction, a), and B2 Configuration (Two Operating Units, b). Numbers in Parenthesis are the Missile Zones and the Second Number is the Relative Missile Density (see Tables 4 and 5). Table 6 lists the Hit Frequency (in Units of Hits/Missile ft^2) for the Different Targets of Plant B.

missile density in the different zones. Warm colors correspond to high relative missile density, and cool colors to low missile density. Green colors are for relative densities close to unity (i.e., missile density comparable to the Plant A analysis). The white structures in the center are the top view of Plant B. Figure 10(a), configuration B1, only includes the buildings of Unit 1 (Unit 2 is assumed under construction). Figure 10(b) displays the buildings for both Units 1 and 2. Configuration B1 is similar to Plant A (with the exception of building 9, which is present in Plant B, but not in Plant A). If the relative missile density was unity in the B1 configuration, then the MIP values for Plant B1 would be expected to be similar to the MIP values for Plant A. In reference to Eq. [20], If the relative missile density of the zones enclosing Plant B1 is higher (lower) than unity, then the MIP would be expected, as a first approximation, to be more than (less than) the Plant A MIP values, although other features of the missile population (missile type and insertion height) may compete with this first order expectation. Actual results are analyzed in the following paragraphs, in comparison to expected results (expectation derived by directly applying Eq. [20]).

Table 6 lists the hit frequency for configurations B1 and B2 in Region I. The frequency of tornados exceeding F'2 intensity is 1.36×10^{-3} 1/yr (see Table 2). With this frequency, the target areas from Table 3, and the hit frequency 1.36×10^{-3} 1/yr, the MIP was computed. The NP-768 report does not include hit frequency per target and per tornado intensity. Instead, the hit frequencies are aggregated over all tornado intensities in excess of F'2. Total values of MIP are listed in Table 6 for configurations B1 and B2, using the exposed wall area and the total exposed area (wall + roof) to normalize the MIP. Table 6 includes columns labeled as MIP(B1)/MIP(A) and MIP(B2)/MIP(A). [The values MIP(A) are listed in Table 2.] Target 8 is not part of Plant A, but it is similar to Target 6. Accordingly, the ratio MIP(B1)/MIP(A) was computed using the Target 6 MIP for Plant A. Likewise, the ratio MIP(B2)/MIP(A) for Targets 10 to 16 was computed using their Plant A similes (e.g., Target 10, containment building of unit 2, is compared to Target 1, containment building of Plant A). The turbine buildings, Targets 9 and 15, are not in Plant A, and this is why the MIP(B2)/MIP(A) ratios are empty in Table 6.

The magnitude of values in the columns MIP(B1)/MIP(A) and MIP(B2)/MIP(A) in Table 6 are expected to correlate to the relative missile densities in Figure 10 (see Eq. [20]). For example, in Figure 10(a), Targets 1 to 5, and Target 7 of Unit 1 are embedded in a zone of relative missile density equal to 1.57. Accordingly, the corresponding MIP(B1) would be expected to be higher than MIP(A), if it was only influenced by a zone of relative missile density equal to 1.57. Targets 1 and 3 do exhibit the expected larger values. It is notable that MIP(B1)/MIP(A) for Target 3 is precisely 1.57. For Target 1, the ratio is 2.46. The higher value of this ratio can be explained due to the proximity of the Unit 2 construction zone (Zone 2), which has relative missile density equal to 10.47 and high missile insertion heights (equal to 100 ft for most missile types). Targets 2 and 5 produce lower MIP(B1) values, which may be due to the other surrounding missile zones of lower relative missile density, and due to the presence of the extra Target 9 building (this building is not in Plant A).

The south wall of Target 4 faces directly missile zones 3 and 4, (relative missile densities equal to 0.72 and 0.4, respectively). The ratio MIP(B1)/MIP(A) is 0.57, which is consistent with the 0.72 and 0.4 values. The largest MIP for B1 is for Target 8. Target 8 is similar to Target 6 of Plant A. The ratio MIP(B1)/MIP(A) = 0.73 compares Target 8 of Plant B1 to Target 6 of Plant A. The 0.73 ratio is consistent with the relative missile density of missile zone 3 (0.72). The anomalous result is the ratio MIP(B1)/MIP(A) = 0.11 for Target 6. If Target 16 is under construction, then Targets 6 and 8 are identical, and identical MIP values would be expected. One explanation on the lack of symmetry of the MIP results is that Target 16 building was possibly included in the B1 TORMIS simulations, protecting Target 6 against missile impacts.

Table 6. Missile Hit Frequencies and MIP for Plant B in B1 and B2 Configurations

Target	Description	Plant B, B1 Configuration				Plant B, B2 Configuration			
		Hit Frequency (Hits/Missile-yr)*	MIP (Hits/Missile-ft^2), Per Exposed Wall Area	MIP (Hits/Missile-ft^2), Per Total Exposed Area	MIP(B1) / MIP(A)	Hit Frequency (Hits/Missile-yr)†	MIP (Hits/Missile-ft^2), Per Exposed Wall Area	MIP (Hits/Missile-ft^2), Per Total Exposed Area	MIP(B2) / MIP(A)
1	Containment 1	1.88E-09	3.49E-11	1.97E-11	2.46	1.52E-08	2.82E-10	1.59E-10	**19.87**
2	Auxiliary Building	5.40E-09	1.15E-10	5.62E-11	0.58	4.82E-09	1.03E-10	5.01E-11	0.52
3	Fuel Handing Building	1.42E-08	4.05E-10	2.60E-10	1.57	8.95E-09	2.55E-10	1.64E-10	0.99
4	Diesel Generator Building	9.85E-09	5.18E-10	3.29E-10	0.57	2.32E-09	1.22E-10	7.76E-11	0.13
5	Waste Processing Building	9.64E-09	1.85E-10	7.42E-11	0.87	1.00E-08	1.92E-10	7.69E-11	0.90
6	Service Water Intake Str. 1-1	2.89E-10	1.33E-10	6.64E-11	**0.11**	1.70E-10	7.82E-11	3.91E-11	0.06
7	Tanks Enclosure	1.58E-09	7.26E-11	4.76E-11	0.21	5.40E-09	2.48E-10	1.63E-10	0.73
8	Service Water Intake Str. 1-2	1.93E-09	8.87E-10	4.44E-10	0.73‡	2.23E-10	1.03E-10	5.13E-11	**0.08**
9	Turbine Building					8.76E-09	1.24E-10	6.87E-11	
10	Containment 2					1.11E-09	2.06E-11	1.16E-11	1.45
11	Auxiliary Building 2					5.95E-09	1.27E-10	6.19E-11	0.64
12	Fuel Handing Building 2					3.44E-09	9.81E-11	6.29E-11	0.38
13	Diesel Generator Building 2					2.75E-09	1.44E-10	9.2E-11	0.16
14	Tanks Enclosure 2					1.82E-09	8.37E-11	5.49E-11	0.24
15	Turbine Building 2					8.95E-09	1.27E-10	7.02E-11	
16	Service Water Intake Structure 2					2.21E-09	4.06E-10	2.26E-10	0.33

*Source: Region I values in NP-768 Table 3-23
†Source: Region I values in NP-768 Table 3-25
‡Since target 8 does not exist in Plant A, this number is normalized to Target 6 of Plant A, which is a similar structure to Target 8 in Plant B

The tornado frequency to compute MIP values is 1.36×10^{-3} 1/yr (frequency of tornados exceeding F'2 intensity). See the last row in Table 2 in this report. Target areas (exposed wall and roof areas) are listed in Table 3. Values of MIP for Plant A are listed in Table 2.

Values of the ratio MIP(B2)/MIP(A) are listed in the last column of Table 6. Targets 1 and 10 (containment buildings for Units 1 and 2) of Plant B are compared to Target 1 of Plant A. Targets 2 and 11 (auxiliary buildings for Units 1 and 2) of Plant B are compared to Target 2 of Plant A, and so forth. The missile distribution in Figure 10 shows that the Units 1 and 2 are surrounded by missile zones of high relative density (zone 1 = 2.40, zone 2 = 1.7, zone 5 = 1.69, zone 6=2.36). If the Unit 2 were not present, the MIP values would be expected to be greater than the MIP values for Plant A. The Unit 2 provides mutual shielding among targets, causing lower MIP values. These competing factors make difficult accurately predicting MIP(Plant B2) on the basis of MIP(Plant A), but some expected and unexpected results can be identified. For example, it is notable that MIP (Target 1) of Plant B2 is much greater than MIP (Target 1) of Plant A. The value MIP(B2)/MIP(A) = 19.87 for Target 1 is unexpected because surrounding missile zones are not of such high relative missile density, and the mutual protection of the two-unit buildings should have lowered MIP(Target 1). It is difficult to identify the reason for such relative large ratio (19.87). It might be due to differences in the missile insertion heights. The ratio MIP(B2)/MIP(A) = 1.45 for Target 10 is reasonable, consistent with the relative missile density of the surrounding zones and mutual protection by Unit 1 and Unit 2 buildings. Other interesting targets are 8 and 16. Target 16 yields the highest MIP. The ratio MIP(B2)/MIP(A) for this target is 0.33 (using Target 6 of Plant A as comparison point). This ratio appears low, because the relative missile density of the surrounding zones is greater than 0.33; however, the different insertion height of missiles also contributes to the final result. The Target 16 is 480-ft distant from Target 5, and 350-ft distant from Target 4. This target appears far from other structures to be shielded against missile hits by the other targets. Nonetheless, the presence of Unit 2 buildings, the low relative missile density in zone 3 (= 0.6), and the different missile insertion heights, appear to cause a decrease in the MIP with respect to Plant A values. The Target 8 ratio is very anomalous, MIP(B2)/MIP(A) = 0.08 (using also Target 6 of Plant A as the comparison target). Figure 10(b) shows that the Target 8 is farther away from other structures than Target 16. It is not clear the cause of the factor of 4 difference between Targets 8 and 16.

Figure 11 displays MIP values for configurations B1 and B2. The scale of Figures 11(a) and (b) is the same as Figure 4(b), to allow for direct visual comparison to Plant A results. Figure 11(c) presents MIP values for B2 configuration in logarithmic scale.

Figure 11(a) is similar to Figure 4(b) for Plant A. The small Target 8 produces the highest MIP. It is surprising Target 6 does not yield a relatively high MIP value (as in Plant A), as is almost identical to Target 8. It is conjectured, as previously stated, that Target 16 was included in the B1 configuration, protecting Target 6 of missile hits; thus explaining the different MIP values. The next highest MIP is for Target 4, in both Plants A and B1. In the B1 case, the magnitude is not as relatively high as in Plant A, because the enclosing missile density is low [missile zone 3, relative missile density = 0.72, see Figure 10(a)]. Target 3 exhibits the next highest MIP. In this case, the MIP is even higher (1.57 times higher) than the Target 3 MIP in Plant A. As previously explained, this is due to the proximity of Target 3 to the missile zone 2 (Unit 2 construction zone), which has the highest missile density in the B1 configuration [relative missile density = 10.47, see Figure 10(a)] and the highest missile insertion height (up to 100 ft). This missile zone 2 also causes the MIP for the containment building, Target 1, to be greater (2.47 times greater, see Table 6) than the corresponding MIP of Plant A. The relative missile densities in Figure 10 correlate to the relative magnitude of the MIP values, and to the MIP values of Plant A [reported in Table 2 and Figure 4(b)].

(a) Configuration B1

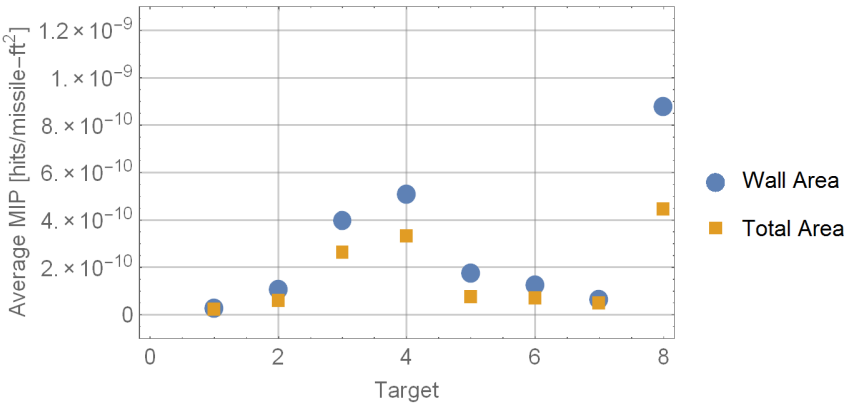

(b) Configuration B2, Linear Scale

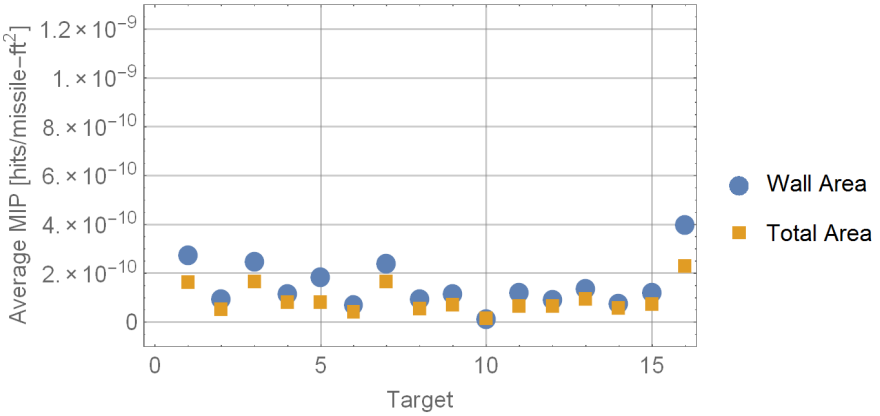

(c) Configuration B2, Logarithmic Scale

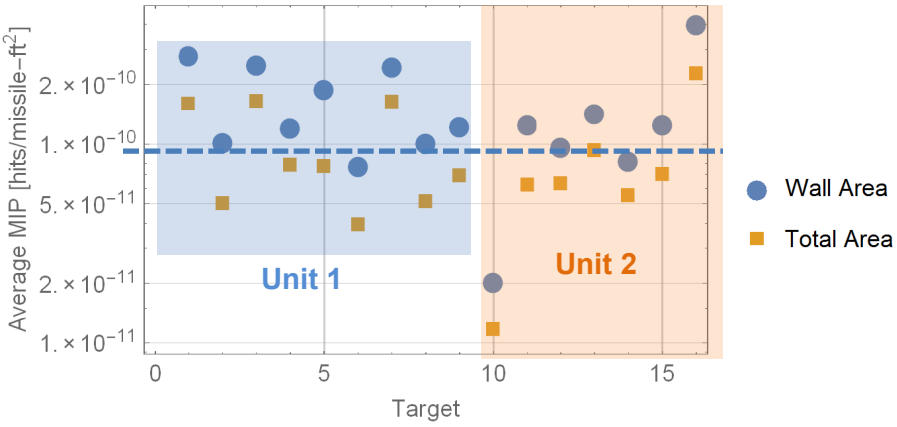

Figure 11. Average MIP for the Different Targets for Configurations B1 (a) and B2 (b and c). In Computing the MIP, Two Normalization Areas Were Considered: Exposed Wall Area and Total Area (Exposed Wall Area + Roof). The Two Alternative MIP Values per Target Are Displayed in the Plots. Consult Table 6 for Data Sources.

In the configuration B2 in Figure 11(b), the highest MIP is Target 16, which is a small and short building, next to Targets 6 and 8, but distant from the other targets. This target is comparable to Target 6 of Plant A. Although far from other buildings, the ratio MIP(B2)/MIP(A) = 0.33 (see Table 6) may indicate that some protection against missile hits is derived by the presence of the other Unit 1 and 2 buildings. The lower missile insertion heights also contribute to the decrease of MIP. Otherwise (i.e., same insertion height as Plant A), the ratio would be expected closer to the relative missile densities of zones 1 (2.40) and 3 [0.60, see Figure 10(b)]. The low value of MIP for Target 8 is an anomaly, given its similarity to Target 16 (in building dimensions, distance to other buildings, and placement in missile zones). Another anomalous MIP is Target 1 (Unit 1 containment building). The MIP is a factor of 20 greater than the MIP for Target 1 in Plant A (see Table 6). Also unexpected is the large difference with respect to the MIP of Target 10 (Unit 2 containment building). It is difficult to explain the high value of the Target 1 MIP compared to Target 10 and Target 1 of Plant A. The different missile insertion heights may have contributed to the different results.

Figure 11(c) displays the same data as Figure 11(b), B2 configuration MIP, but in logarithmic scale. The majority of the MIP values normalized with respect to the exposed wall area are around 10^{-10} hits/missile-ft^2 (see the dotted line). The exceptions, in the Unit 1 buildings, are Targets 1, 3, 5, and 7. The Target 1 MIP value was identified as an anomaly in the previous paragraphs. The Targets 3 and 7 are analogous to Targets 12 and 14 of Unit 2, yet the former targets yield higher MIP values. An explanation for the high MIP values for Targets 3, 5, and 7 is their location, close to missile zone 6 (relative missile density = 2.36), which is the zone of second highest missile density. On the other hand, Targets 12 and 14 are close to missile zone 2 (relative missile density = 1.70). The different densities for zones 2 and 6 make the system asymmetric. This asymmetry helps explaining why the MIP for Targets 3 and 7 is greater than the MIP for Targets 12 and 14.

The discussion supports the conclusion from the previous section. The MIP correlates to the missile density. In other words, the MIP for a non-uniform spread can be approximated as

$$\overline{MIP}_i = \frac{\bar{\rho}_m}{\rho_{average}} \, MIP_i^{NP} \qquad [28]$$

where $\bar{\rho}_m$ is the average missile density of zones close to missile i, and $\rho_{average}$ is computed as the ratio of the number of missiles and the $L\,W$ area (see Eq. [22]).

The total number of hits on a target is estimated using the complete missile count over the whole $L\,W$ area. For example, 5,000 missiles were considered in the B1 configuration analysis. Thus, the number of missile hits on target i in the B1 configuration would be estimated as

$$h_i = 5{,}000\,\overline{MIP}_i \times (\text{area of target}) = 5{,}000\,\frac{\bar{\rho}_m}{\rho_{average}}\,MIP_i^{NP} \times (\text{area of target}) \qquad [29]$$

Since $\rho_{average} = 5{,}000 \text{ missiles}/\,L\,W$, Eq. [29] can then be rewritten as

$$h_i = MIP_i^{NP}\,\bar{\rho}_m\,L\,W \;\times (\text{area of target}) \qquad [30]$$

This equation is the same as Eq. [25]. Therefore, the analysis of Plant B confirms the reasonableness of the alternative Eq. [25] to compute the number of hits, with $\bar{\rho}_m$ interpreted as an average nearby missile density. Alternatively, the MIP can be adjusted using Eq. [28], and the industry equation, Eq. [12] can still be used to estimate the number of hits (with the adjusted MIP).

The nuclear energy industry proposed the notion of a missile-free zone to decrease the number of missile hits. Equation [30] is consistent with the missile-free zone notion. If a large enough missile-free zone is proposed (keeping potential missiles very distant from a target), then $\bar{\rho}_m = 0$, and Eq. [30] would predict 0 hits on targets.

2.6 Probability of Structure Damage Given a Missile Hit

In this section the following questions are examined

- Is there information in NP-768 that may allow justifying taking credit for the structural strength of targets against missile strikes?

- What is a reasonable reference value of MIP to be used in generic tornado hazard analyses?

We concluded that it is difficult to take credit for the structural strength of components against hits. It is not possible to generalize computations based on concrete and specific features of the missile population. However, the NP-768 data indicate that missiles hitting well above ground carry more kinetic energy than hits close to the ground. This information is useful to selecting a reference MIP, which may be a reasonable upper bound. It may not be necessary to seek a strict upper bound computed using small targets close to the ground; as such targets may mostly be impacted by low energy missiles. The analysis in support of this conclusion is provided as follows.

The nuclear energy industry proposes to assume component failure if hit by a tornado-generated missile, independently of the energy of the impacting missile. This is clearly a conservative approach. In this section, the data from NP-768 are briefly analyzed to identify the possibility of taking credit for structural capacity against missile impact. All of the targets in the NP-768 analysis are reinforced concrete barriers of 4,000 psi compressive strength. All targets were assumed to be of the same concrete penetrability factor (K_b=163) and of the same scabbing thickness reduction factor (R_s=0.97). Target 1 is 36-inch thick in the cylinder wall and 24-inch thick in the dome. The wall of Targets 2 to 5 is 18-inch thick, and Target 6 and 7 are 12-inch thick. The NP-768 tracked the frequency of missile hits (per missile) with at least 6 inches of scabbing or penetration damage, and denoted this frequency as D_L. The ratio D_L/H is interpreted as the conditional probability of damage in excess of 6 inches given a missile hit.

Figure 12 shows a plot of the ratio D_L/H as a function of the F' tornado scale and target, for Plant A. The source of the data is NP-768 Tables 3-8 to 3-14, Region I. It was verified that Region II or III data would yield practically the same ratios, with differences attributable to statistical artifacts. The target curves in Figure 12 exhibit an expected increasing trend with tornado intensity. Higher intensity tornados generate missiles of higher kinetic energy (because of higher wind speed) that can cause more damage. The Target 6 includes only one point at F'6 in Figure 12; for lower tornado magnitudes there was no record of any hit exceeding 6-inch damage. Target 2 exhibited the largest conditional probability of damage, with an anomalous spike at F'3.

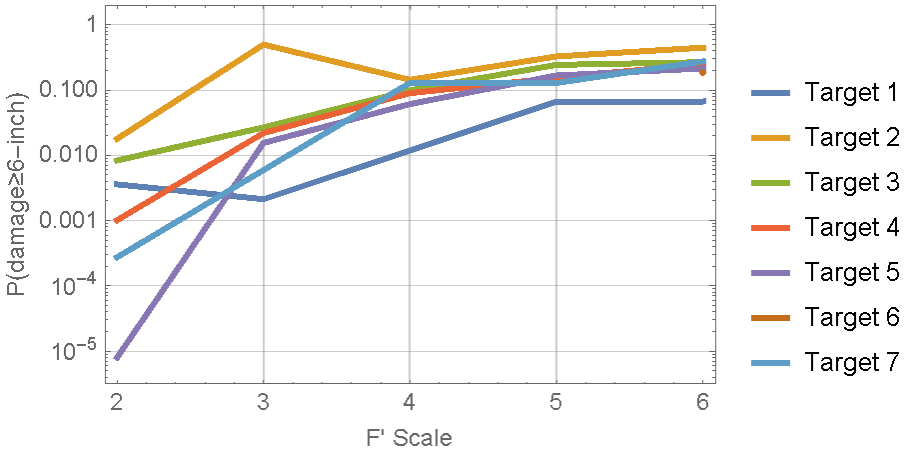

Figure 12. Ratio D_L/H Versus F' Scale and Target for Plant A. The Ratio D_L/H Is Interpreted as the Conditional Probability for a Missile to Cause Damage in Excess of 6 Inches, Given a Hit to a Target. The Data Source Are NP-768, Tables 3-8 to 3-14.

Figure 13 is provided to explore the reason of the difference in conditional probability of damage among the various targets. The total conditional probability of missile damage in excess of 6 inches, P(damage > 6 inches), was computed as the sum of D_L over all F' scales divided by the total hit frequency per missile (sum of H over all F' scales). Figure 13 includes plots of P(damage > 6 inches) versus target and versus building height for Plants A, B1 and B2. The plots on the right-hand side of Figure 13, P(damage > 6 inches) versus building height, indicate that taller targets tend to exhibit larger P(damage > 6 inches). The correlation coefficient between P(damage > 6 inches) and the building height is high and positive, confirming the visual trend that P(damage > 6 inches) tends to increase with building height. The increasing trends indicate that the taller buildings are impacted by missile hits carrying higher kinetic energy and causing deeper damage. (The exception to this interpretation is Target 1 in Plant A. For some reason, this tallest target received not only few hits, but most of those hits were low energy.) In Section 2.2 it was demonstrated that shorter buildings tend to exhibit higher MIP. In this section it is argued that although the shorter buildings get more hits, most of those hits are low energy, and only few will cause component damage. On the other hand, the tall buildings may be impacted by hits carrying more kinetic energy. Hits impacting zones well above ground are more likely to damage or fail components or structures. Note for example in Figure 13, in the B2 configuration, almost all of the hits to containment buildings (Targets 1 and 10) cause damage in excess of 6 inches. Therefore, based on the NP-768 data, it is concluded that the failure likelihood of a target hit by a tornado-generated missile is a function of the height or vertical placement of that target. Taller targets are more likely to fail if struck by a missile.

On the question of the reasonableness of accounting for the strength of a target, it is difficult to generalize data in NP-768. The targets are all made of concrete of the same properties. If 6-inch damage were selected as failure criterion, then no credit should be assigned to tall concrete structures. Most of the targets in the B1 and B2 configuration in Figure 13 yield P(damage > 6 inches) in excess of 0.1 (i.e., not far from 1); thus, not taking credit for the strength of the structure would be reasonable in the Plant B examples. It is recognized that targets of interest can be made of materials other than concrete (e.g. steel), and the failure criterion for those other targets would need to be properly established. Based on the NP-768 analysis, it can only be inferred that targets located in tall places are more likely to fail if hit by a missile.

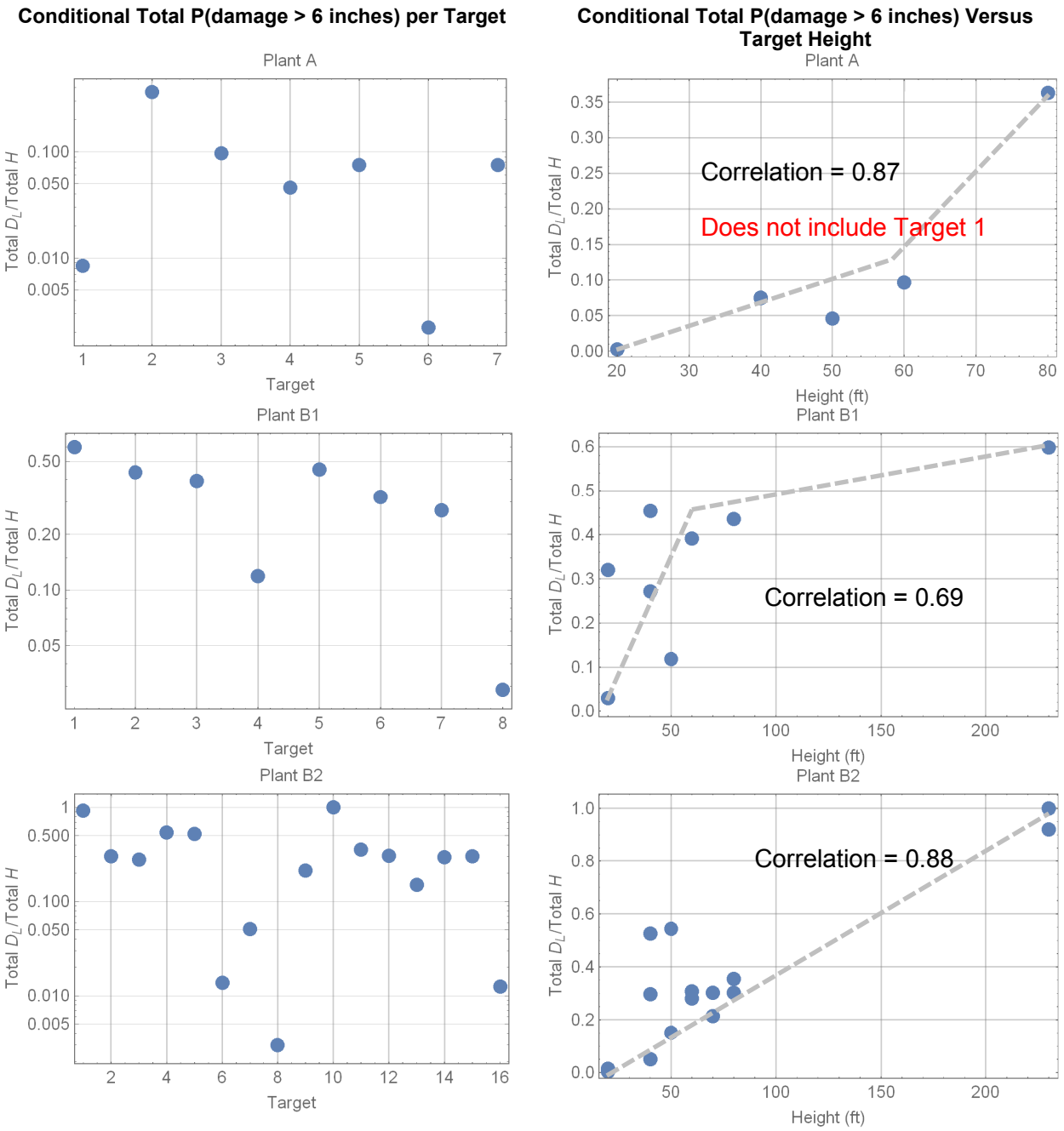

Figure 13. Ratio Total D_L/Total H Versus Target Number and Versus Target Height. There Is a Clear Positive Correlation Between Total D_L/Total H and the Target Height.

Failure of a structure or component depends not only on the tornado hazard (wind speed), but also on the missile composition. The complete hazard against structures is defined by the tornado hazard and the missile population features. Thus, it does not appear reasonable to assign a generic conditional failure probability of a structure or component given a missile hit, when this probability is dependent on features of the missile population (which change from site to site). At this point, not taking credit for the strength of the target is a reasonable and defensible approach.

2.7 Selection of a Reference MIP

This section addresses the question

- What is a reasonable reference value of MIP to be used in generic tornado hazard analyses?

Based on analyses in this report, the MIP is dependent on factors such as mutual shielding, target geometry, and distance above the floor of the target. A defensible, generic, MIP would be expected to bound of site-specific MIPs, and be independent on the configuration of buildings on a site. The MIP for Targets 6 and 4 in Plant A appear relatively bounding and are proposed to be considered for reference values. Other alternatives could be considered provided dependencies, such as those discussed in this report, do not result in greatly underestimating the number of missile hits and hit frequencies in a safety-related component. In this section, a comparison is made to MIP values reported in Appendix G of NUREG/CR-4710 (Boissonnade and W.L. Ferrell, 1987). A discussion is provided on reasonable reference MIP values using findings in this report.

In Appendix G of NUREG/CR 4710 (Boissonnade and W.L. Ferrell, 1987), a normalized tornado missile impact parameter, Ψ, is defined equivalently to the MIP definition in Eq. [6]. Quantiles of Ψ, computed as an average of buildings of Plants A and B1, are reported elsewhere (Julka, 2016). Table 7 summarizes values of MIP, normalized by the total exposed target area (exposed wall + roof), sorted by increasing values of MIP, for Plants A and B1. Each MIP value is averaged over all of tornado intensities. The "accumulated" area column is the sum of the areas in the previous rows. For example, the accumulated area entry on the last row of the Plant A section in Table 7, 3.41×10^5 ft^2, is the total exposed area of all targets. The relative accumulated area is the ratio of the accumulated area and the total exposed area. The relative accumulated area column can be interpreted as the corresponding quantile of a cumulative density function. For example, for Plant A the 0.21 quantile of the MIP is 8×10^{-12} hits/missile-ft^2, the 0.49 quantile is 8.55×10^{-11} hits/missile-ft^2, and so forth. The cumulative density functions so built are displayed in Figure 14(a). The MIP values compare well to Ψ values. The average MIP of the A-B1 system is 1.21×10^{-10} hits/missile-ft^2, while the average of Ψ from the values reported by Julka (2016) is 1.23×10^{-10} hits/missile-ft^2. Therefore, MIP values computed in this report are consistent with Ψ values reported elsewhere. The distributions in Figure 14(a) convey variability in the MIP due to the placement of building (i.e., mutual shielding) and height of buildings.

Figure 14(b) compares the A-B1 average in Figure 14(a) to cumulative density functions for the different targets constructed with data in Table 2. The approach to compute density functions for the seven targets is identical to the approach implemented in Table 7, but using the frequencies in Table 2 to compute weight values instead of the areas in Table 7. For any target, the distributions in Figure 14(b) exhibit variability in the MIP due to different tornado magnitudes.

Table 7. Missile Impact Probability for Plants A and B1 (Normalized by the Total Exposed Area). The Relative Accumulated Area Is Interpreted as a Quantile of the Cumulative Probability Density Function of the MIP.

Plant A					Plant B1				
Target	MIP (hits/missile-ft^2)	Total Exposed Area (ft^2)	Accumulated Area (ft^2)	Relative Accumulated Area	Target	MIP (hits/missile-ft^2)	Total Exposed Area (ft^2)	Accumulated Area (ft^2)	Relative Accumulated Area
1	8.00E-12	7.04E+04	7.04E+04	0.21	1	1.96E-11	7.04E+04	7.04E+04	0.21
5	8.55E-11	9.56E+04	1.66E+05	0.49	7	4.76E-11	2.44E+04	9.48E+04	0.29
2	1.10E-10	8.05E+04	2.46E+05	0.72	2	5.62E-11	7.07E+04	1.65E+05	0.50
3	1.65E-10	4.02E+04	2.87E+05	0.84	6	6.64E-11	3.20E+03	1.69E+05	0.51
7	2.24E-10	2.44E+04	3.11E+05	0.91	5	7.41E-11	9.56E+04	2.64E+05	0.80
4	5.82E-10	2.20E+04	3.33E+05	0.98	3	2.60E-10	4.02E+04	3.04E+05	0.92
6	7.34E-10	8.00E+03	3.41E+05	1.00	4	3.29E-10	2.20E+04	3.26E+05	0.99
					8	4.43E-10	3.20E+03	3.30E+05	1.00

Total exposed area = exposed wall area + roof area
Accumulated area: sum of area of all targets in previous rows
Relative accumulated area = accumulated area / total area of all targets. This quantity is interpreted as the quantile of the MIP.
Average MIP of Plant A: 1.42×10^{-10} hits/(missile-ft^2)
Average MIP of Plant B1: 9.99×10^{-11} hits/(missile-ft^2)
Average MIP of Plants A and B1: 1.21×10^{-10} hits/(missile-ft^2)
Average of Ψ: 1.23×10^{-10} hits/(missile-ft^2)

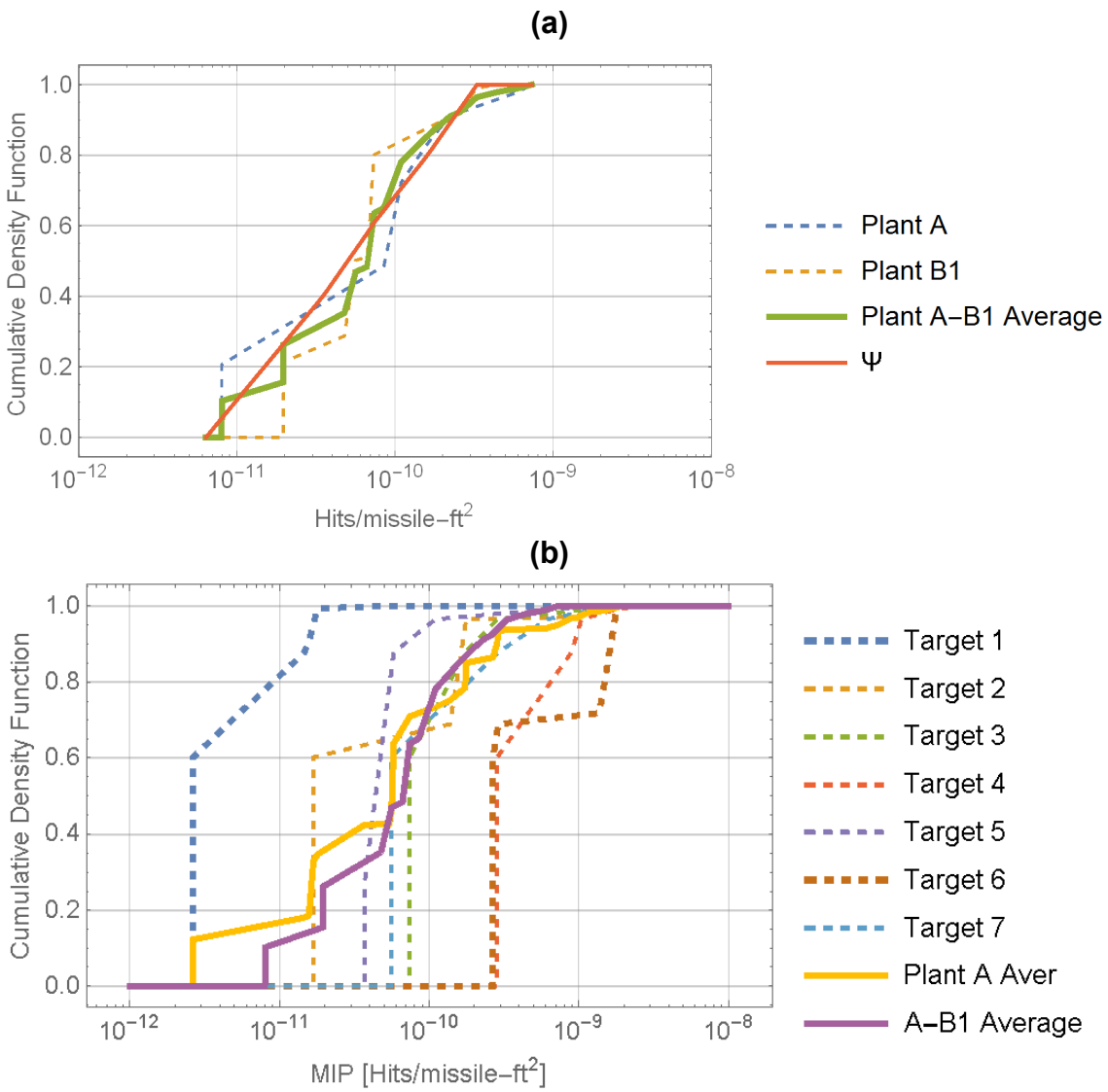

Figure 14. (a) Comparison of Average MIP of Plants A and B1 to Ψ Values in Julka (2016). (b) Comparison of Average MIP of Plants A and B1 to Plant A Targets Varying as Function of F'.

The continuous yellow curve (labeled as Plant A average) is the average of all of the distribution functions of the seven targets, using the target exposed area as weight to compute the average. Thus, the yellow curve exhibits the variability in the MIP due to (i) relative shielding among targets, (ii) height of targets, and (iii) tornado magnitudes. By contrast, the continuous purple curve labeled as A-B1 average [same as the Plant A-B1 Average in Figure 14(a)] only displays variability due to the factors (i) and (ii) and, thus, the spread of the purple curve is expectedly narrower than the yellow curve average.

An aspect not reflected in the variability of the cumulative density functions in Figure 14(b) is variability of the MIP within a target. For example, with reference to Figure 3 (a schematic of the south wall of Target 4), if the target area of reference to compute the MIP was smaller than the total exposed surface (e.g., rectangles 1 and 2 in Figure 3), then the MIP would exhibit larger variability. With smaller surface segments, the distribution functions would be expected to

exhibit tails both spanning to the right and the left of the dotted line curves in Figure 14(b). In other words, larger and lower values of the MIP can be computed just by selecting smaller surface segments than the total target exposed area. Appendix G of NUREG/CR–4710 reports higher and lower values of Ψ (equivalent to MIP) than in Figure 14(b), for small targets, which is expected. Small targets at low locations (e.g., just above ground) can yield higher MIP values.

What should be a reasonably representative MIP value to be used, in general, to estimate a number of missile hits in other facilities? The lowest MIP values are for Target 1 (tallest building, completely protected by other targets against hits in the lower parts of the containment building). Potential targets of interest to utilities may not be located as high as the exposed surface of Target 1. Intermediate MIP values correspond to Targets 2, 3, 5, and 7. Those MIP values account for mutual protection by the relative placement of the power plant buildings. A different configuration of buildings (e.g., different number of buildings of varying geometry and placement) would yield different MIP values. Care should be exercised in using MIP values for Targets 2, 3, 5, and 7 in analyses of different plants, as those values may not correspond to the configuration of buildings of interest. The largest MIP values for Plant A correspond to Targets 4 and 6 [as shown in Figure 14(b)]. Those targets are short and distant from other targets. In particular, it is hypothesized that TORMIS runs with solely Target 6 would yield comparable MIP values to Target 6 in the Plant A system. Thus, the Target 6 MIP is perceived less dependent or weakly dependent on the configuration of the power plant buildings. Given this potential independence on building configuration, it appears reasonable to consider Targets 6 and 4 to define reference MIP values that could be used in general tornado hazard analyses. Nonetheless, we recommend verifying that the MIP for Target 6 is independent of the building configuration.

The Target 4 and 6 MIP values are relatively bounding. However, as previously stated, the MIP can increase if smaller targets are considered, or smaller surface segments within a target are accounted for. For example, computing the MIP in surface segments of the south wall of Target 4 (e.g., rectangle 2 in Figure 3) would yield higher MIP values. However, as discussed in Section 2.6 that hits well above ground (i.e., hits in taller parts of buildings) tend to be more energetic than lower hits close to the ground. Therefore, small targets placed just above ground are less likely to lead to component failure if hit by a missile. Small targets placed in taller parts of buildings are more likely to be damaged if hit by a missile, but the hit frequency would be lower. For those reasons, selecting the total exposed area MIP averages for Targets 4 or 6 represents a compromise between targets that could experience a relatively high number of missile hits per unit of area, and identification of missiles with enough energy to cause component failure. Selecting as reference small targets or surface segments of targets may be overly conservative, as surface segments with high hit density may also be segments affected by low-energy missiles.

3 CONCLUSIONS

The nuclear energy industry is proposing to define a tornado-generate missile impact probability (MIP) based on data in the NP-768 report (EPRI, 1978) as a basis to estimate the hit frequency on targets at a nuclear power plant. The MIP is the number of hits per missile, per unit of target area, given a tornado at or near a site. The MIP would be linearly scaled with the tornado frequency, the area of the component, and the number of missiles in the site to estimate a hit frequency. The hit frequency would be interpreted as the frequency of failure of a safety-relevant component (i.e., the component would be assumed failed if hit by a tornado-generated missile), to be input into a detailed PRA to compute the CDF and LERF. The MIP concept was analyzed in this report. The scaling approach was found defensible, but additional verification and adjustments are needed in several areas.

Based on the NP-768 data, the missile hit frequency is proportional to the tornado frequency. In TORMIS, tornados of the same intensity cause the same consequence (e.g., same number of missile hits of the same kinetic energy), independently of the tornado region. This causes the MIP to be independent of the numeric value of the tornado frequency. The nuclear energy industry approach for estimating the target hit frequency as linearly proportional to the tornado frequency is defensible. A consequence of this finding is that the same MIP values would be derived using TORMIS runs that consider a tornado point-strike frequency or area-strike frequency.

The MIP is a function of (i) the relative placement of targets and power plant configuration, (ii) the height of targets, and (iii) the magnitude of the tornado. Because of these dependencies, care should be exercised in defining a representative MIP to use in general analyses. Based on the analyses described in this report we recommend using MIP values of isolated targets (targets distant to other buildings in the plant) to define a reference MIP (e.g., Target 6 of Plant A in the NP-768 analysis), because the MIP of isolated targets is independent or weakly-dependent of the configuration of buildings. We also recommend additional TORMIS runs to verify that the MIP of a lone target is the same as the MIP of a target far from other buildings.

The hit density (number of hits per unit of target area) is a function of the vertical position of the target. The containment building (Target 1) is only exposed in the upper parts of the building and the dome. This building exhibited the smallest number of hits per unit of area. The service water intake structure (Target 6) is the shortest building and most distant from the other buildings in the Plant A. This building exhibited the largest number of hits per unit of area. It is explicitly stated in NP-768 that few hits were recorded in the roofs of the buildings. Accordingly, it is reasonable to use the exposed wall area as the reference area of the target (and ignore the roof, because it only receives few hits, if at all). Computing the MIP using the total exposed area (wall + roof) produces values that are approximately a factor 0.6 smaller than the alternative that ignores the roof. Given other uncertainties in the analysis, this correction of "exposed wall" versus "exposed wall + roof" is not considered relevant.

The MIP is a function of the missile spread. The NP-768 considered a missile spread over a rectangular area of dimensions 4,640 ft × 5,000 ft (= 2.32×10^7 ft^2). This area is an important aspect of the NP-768 analysis. Hits to a target are dominated by missiles initially located near the target. Selecting a different reference area (different than 2.32×10^7 ft^2) in the numerical TORMIS analyses may not necessarily change the absolute number of hits to a target, but will change the number hits per missile and the MIP. Accordingly, a change is needed in the scaling approach to ensure that a consistent number of missile hits is derived, independently of

the reference missile area employed in the TORMIS runs. Also, the NP-768 TORMIS analysis of the Plant A configuration considered a uniform missile spread. Missile surveys are most likely to identify clusters of missiles spread over different footprints (i.e., the missile distribution would not be uniform). An example is presented in Figure 7 showing that, unless the missile spread footprint is accounted for, the number of missile hits to a target and the corresponding hit frequency can be underestimated using the simple scaling approach proposed by the nuclear energy industry. The MIP is proposed to be corrected as

$$\overline{MIP} = \frac{\bar{\rho}_m}{\rho_{average}} MIP^{NP} \quad [31]$$

where $\overline{MIP}$ is the corrected value, MIP^{NP} is a value based on data in NP-768, $\bar{\rho}_m$ is an average missile density (number of missiles per unit of footprint area). This average may be computed considering clusters of missiles close to the target and the actual footprint area of those clusters. Alternatively, $\bar{\rho}_m$ may be the largest density of relevant missile clusters. The quantity $\rho_{average}$ is computed as

$$\rho_{average} = \frac{\text{number of missiles}}{2.37 \times 10^7 \, ft^2} \quad [32]$$

The correction in Eq. [31] explicitly accounts for the NP-768 area of analysis. For example, if the missiles were spread over an area equal to 0.1 of the NP-768 area (i.e., 2.32×10^6 ft^2), then $\overline{MIP} = 10\, MIP^{NP}$. This correction can be very conservative, especially when the missile cluster is far from the target. To refine the correction, additional TORMIS runs would be needed to establish a dependence of the MIP on the distance of the missile cluster to the target. The information available in NP-768 is not sufficient to define a distance-dependent correction.

The NP-768 tabulated the frequency per missile of hits causing damage in excess of 6 inches to the concrete structures. With such information, the conditional probability for a hit to damage a concrete target by more than 6 inches, given a missile hit to the target, was estimated. A clear correlation between the building height and this conditional probability was identified. For example, for Plants B1 and B2 in the NP-768 analysis the majority or all of the hits impacting the containment buildings (Targets 1 and 10, the tallest targets) cause damage in excess of 6 inches. On the other hand, 10 percent (or less) of the hits to the shortest buildings (Targets 6, 8, and 16) cause penetrations exceeding 6 inches. Therefore, it is inferred that hits to sections of targets well above ground are more likely to cause damage to the structures than low hits close to the ground. This correlation is inverse to the missile hit density (number of hits per unit of target area): the hit density is higher for shorter buildings. These inverse correlations suggest it is reasonable to select the MIP for Targets 4 or 6 as representative MIPs to use in general analyses. Smaller targets, isolated from other targets, located just above ground, may yield larger MIP values. Those alternative MIP values may be too conservative: the associated missile hits would be expected to be of low kinetic energy and less likely to fail a structure or component.

There is currently not enough information on component fragility to justify taking credit for the strength of a structure in case of a missile hit. For example, it is challenging to assert in general that one in every ten hits will be energetic enough to fail a steel door of specific dimensions, for a given tornado intensity. The tornado hazard is a combination of the tornado intensity and features of the missile population (e.g., missile mass, material, dimensions and aspect ratio, insertion heights), which are variable from site to size. If true than one in every 10 hits causes

failure of the steel door in a particular site, such conclusion cannot be directly applied to other sites with different missile populations. Therefore, at this stage, we considered it reasonable to equating hit frequency with component failure frequency.

The NP-768 report includes informative data to justify use of the MIP concept and scaling approach to estimate the frequency of initiating events. The objective of the NP-768 report was estimating hit frequencies and frequencies of energetic hits. To define a general MIP, it would have been more informative to analyze simple systems, such as lone targets and examine independently effects of changes to (i) target geometry, (ii) missile cluster footprints, (iii) distance of missile clusters to a target, (iv) missile population features. In general, we considered the MIP concept defensible. However, additional work is necessary to address the problem of missile clusters of variable spread and variable distance to targets. Absent detailed information, correction factors proposed in this report may be used to adjust the MIP as a function of the missile cluster spread; however, we recognize that those correction factors may be overly conservative in instances of distant missile clusters to targets. Those adjustment factors support the concept of missile free zones near critical targets. Adopting missile-free zones may significantly reduce estimates in missile hit frequencies. Additional work is also needed to define MIP values that are independent of the building configuration. It is hypothesized that the MIP for Target 6 in Plant A is far enough to be affected by the configuration of the other buildings, but additional TORMIS runs would be needed to confirm this observation.

4 REFERENCES

EPRI. "Tornado Missile Risk Analysis." Report NP-768. Electric Power Research Institute: Washington DC. May,
1978. http://www.epri.com/abstracts/Pages/ProductAbstract.aspx?ProductId=NP-768

Calvert Cliffs Nuclear Power Plant. "Probabilistic Risk Assessment Evaluation of Tornado-Generated Missile Impact on the Calvert Cliffs Nuclear Power Plant Emergency Diesel Generator Engine Air Intake and Exhaust." Attachment to letter by Robert E. Denton to the U.S. NRC dated October 13, 1994, of subject *Calvert Cliffs Nuclear Power Plant Units Nos. 1 & 2; Docket Nos. 50-317 & 50-318, Use of NUREG-0800 Standard Review Plan Guidance in Evaluating the Need for Tornado-Generated Missile Barriers*. Baltimore Gas and Electric Company, Calvert Cliffs Nuclear Power Plant: Lusby, Maryland. 1994.

Boissonnade A.C. and W.L. Ferrell. "External Wind Analysis for the St. Lucie Nuclear Power Plant." Appendix G in NUREG/CR–4710, "Shutdown Decay Heat Removal Analysis of a Combustion Engineering 2-Loop Pressurized Water Reactor, Case Study" by W.R. Cramond, D.M. Ericson, and G.A. Sander. Washington, DC: U.S. Nuclear Regulatory Commission. August 1987. SAND 86-1797.

Julka, A. "NUREG 4710 Ψ [psi] Values." Presentation during the January 13, 2016 Public Meeting Between the U.S. Nuclear Regulatory Commission Staff and Stakeholders to Discuss Tornado Impact Parameter. Washington, DC: U.S. Nuclear Regulatory Commission. January 2016. (ML16012A082; meeting summary record available at ML16035A033)

Montgomery, B. "Tornado Missile Risk Evaluator (TMRE)." Presentation during the March 23, 2016 Public Meeting Between the U.S. Nuclear Regulatory Commission Staff and Stakeholders titled *Tornado-Generated Missile Simplified Risk Analysis Table Top Exercise*. Washington, DC: U.S. Nuclear Regulatory Commission. March 21, 2016. (ML16081A399)

Ramsdell,Jr., J.V. and J.P. Rishel. "Tornado Climatology of the Contiguous United States." NUREG/CR–4461, Rev. 2, and PNNL-15112, Rev. 1. Washington, DC: U.S. Nuclear Regulatory Commission. February 2007. (ML070810400)